(12) **United States Patent**

He et al.

(10) **Patent No.:** **US 9,812,736 B2**

(45) **Date of Patent:** **Nov. 7, 2017**

(54) **LITHIUM-SELENIUM SECONDARY BATTERIES HAVING NON-FLAMMABLE ELECTROLYTE**

(71) Applicant: **Nanotek Instruments, Inc.**, Dayton, OH (US)

(72) Inventors: **Hui He**, Beavercreek, OH (US); **Bor Z. Jang**, Centerville, OH (US); **Yanbo Wang**, Huber Heights, OH (US); **Aruna Zhamu**, Centerville, OH (US)

(73) Assignee: **Nanotek Instruments, Inc.**, Dayton, OH (US)

(*) Notice: Subject to any disclaimer, the term of this patent is extended or adjusted under 35 U.S.C. 154(b) by 41 days.

(21) Appl. No.: **13/987,785**

(22) Filed: **Sep. 3, 2013**

(65) **Prior Publication Data**

US 2015/0064575 A1 Mar. 5, 2015

(51) **Int. Cl.**

H01M 10/0569	(2010.01)
H01M 10/0568	(2010.01)
H01M 10/052	(2010.01)
H01M 4/62	(2006.01)
H01M 4/38	(2006.01)

(52) **U.S. Cl.**

CPC *H01M 10/0568* (2013.01); *H01M 4/625* (2013.01); *H01M 10/052* (2013.01); *H01M 4/38* (2013.01); *H01M 10/0569* (2013.01); *Y02T 10/7011* (2013.01)

(58) **Field of Classification Search**

CPC H01M 10/052; H01M 10/0568

See application file for complete search history.

(56) **References Cited**

U.S. PATENT DOCUMENTS

2,798,878 A	7/1957	Hummers	
2004/0241551 A1*	12/2004	Nakamura et al.	.... 429/303

2005/0271574 A1	12/2005	Jang et al.	
2009/0246625 A1*	10/2009	Lu	.... 429/207
2012/0225352 A1*	9/2012	Abouimrane	.... H01B 1/18
			429/211

FOREIGN PATENT DOCUMENTS

CA	2847617	*	3/2014
JP	2005243321	*	9/2005
JP	2007109698	*	4/2007

OTHER PUBLICATIONS

U.S. Appl. No. 10/858,814, filed Jun. 3, 2004, B Z Jang, et al.
Chao Luo, et al. "Selenium@Mesoporous Carbon Composite with Superior Lithium and Sodium Storage Capacity," ACS Nano, Article ASAP, DOI: 10.1021/nn403108w.
Luo et al., "Selenium@Mesoporous Carbon Composite with Superior Lithium and Sodium Storage Capacity" ACS Nano, Article ASAP, DOI: 10.1021/nn403108w.

* cited by examiner

Primary Examiner — Ula C Ruddock
Assistant Examiner — Thomas Parsons

(57) **ABSTRACT**

A rechargeable lithium-selenium cell comprising a cathode having a cathode active material selected from Se or Se_xS_y (x/y ratio=0.01 to 100), an anode having an anode active material, a porous separator electronically separating the anode and the cathode, a non-flammable quasi-solid electrolyte in contact with the cathode and the anode, wherein the electrolyte contains a lithium salt dissolved in a first organic liquid solvent with a lithium salt concentration sufficiently high (at least 2.0 M, more preferably >3.0 M) so that the electrolyte exhibits a vapor pressure less than 0.01 kPa when measured at 20° C., a flash point at least 20 degrees Celsius higher than the flash point of the first organic liquid solvent alone, a flash point higher than 150° C., or no flash point. This battery cell is non-flammable and safe, has a long cycle life, high capacity, and high energy density.
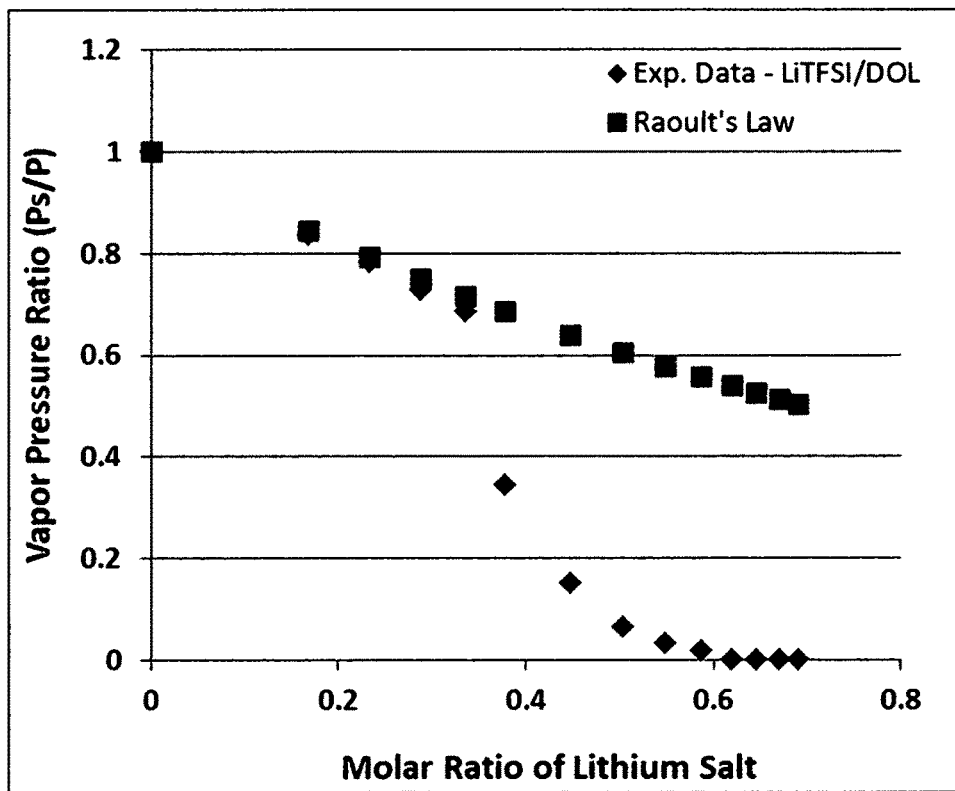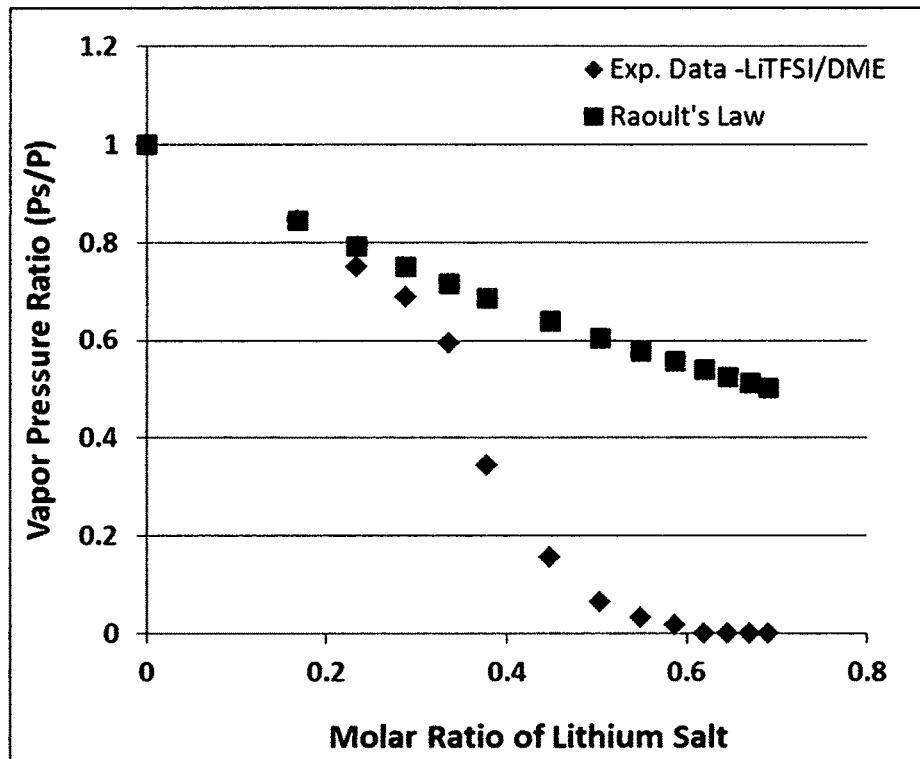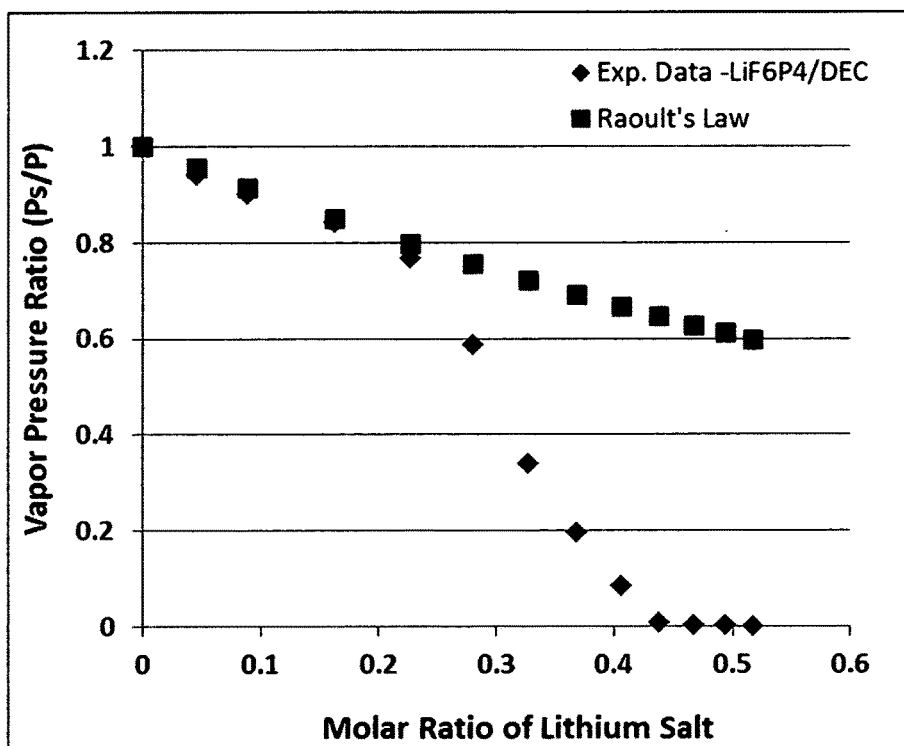
18 Claims, 12 Drawing Sheets

FIG. 1

FIG. 2

FIG. 3
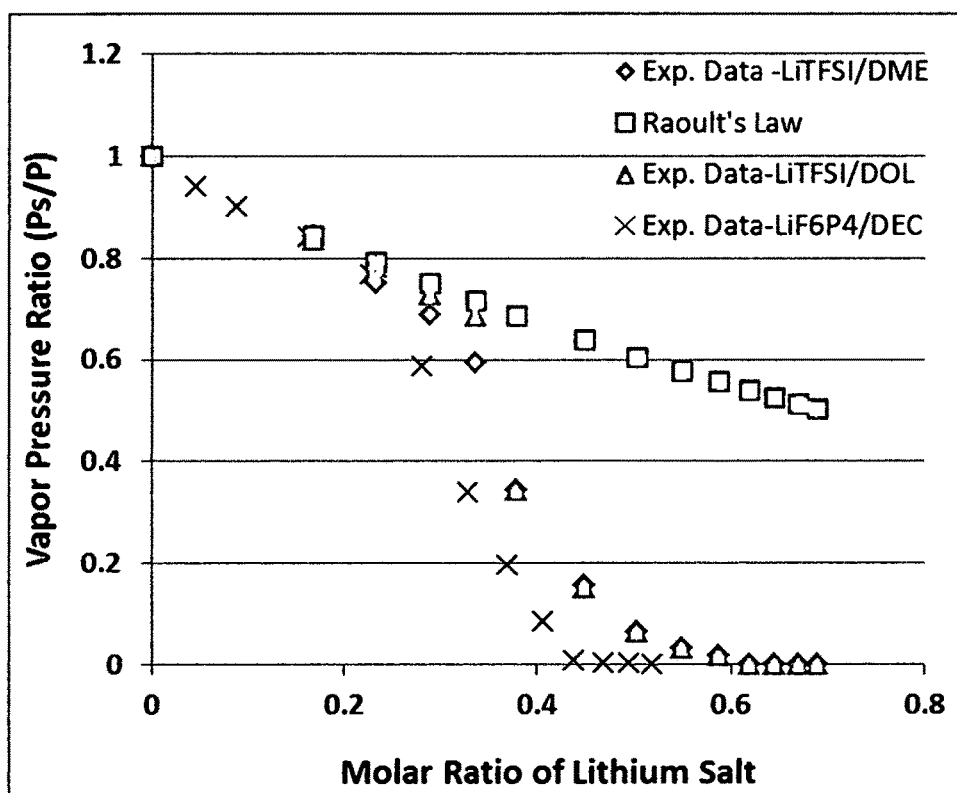
FIG. 4
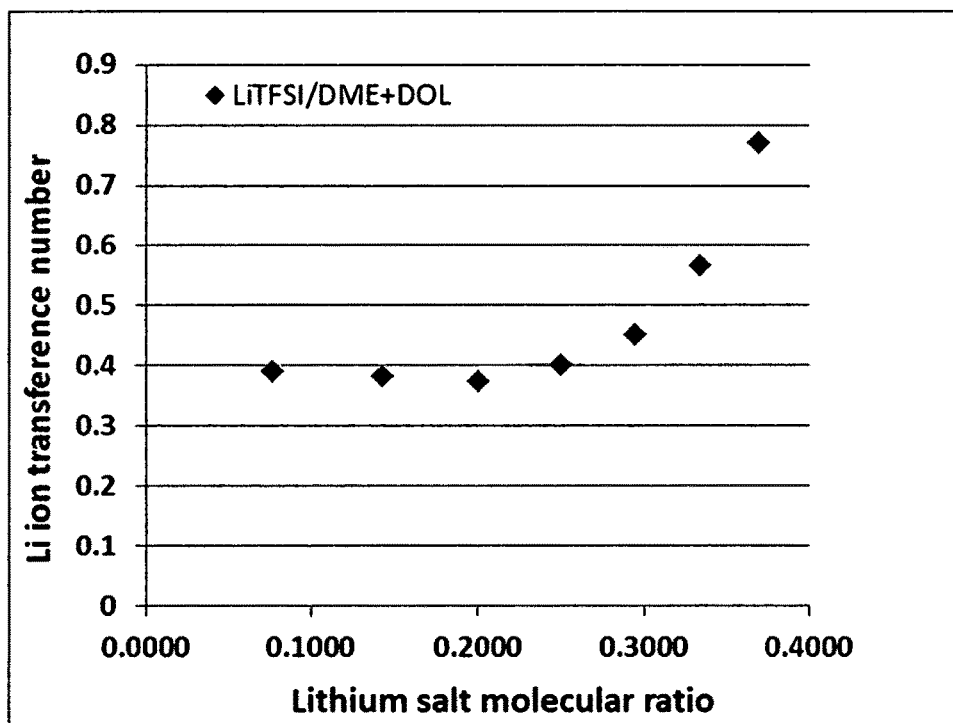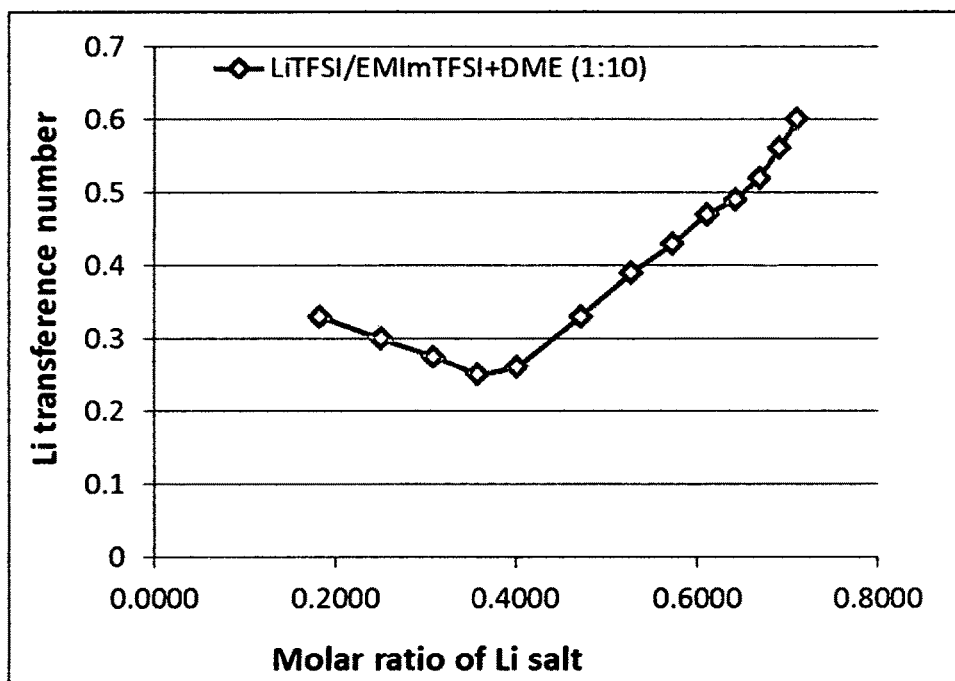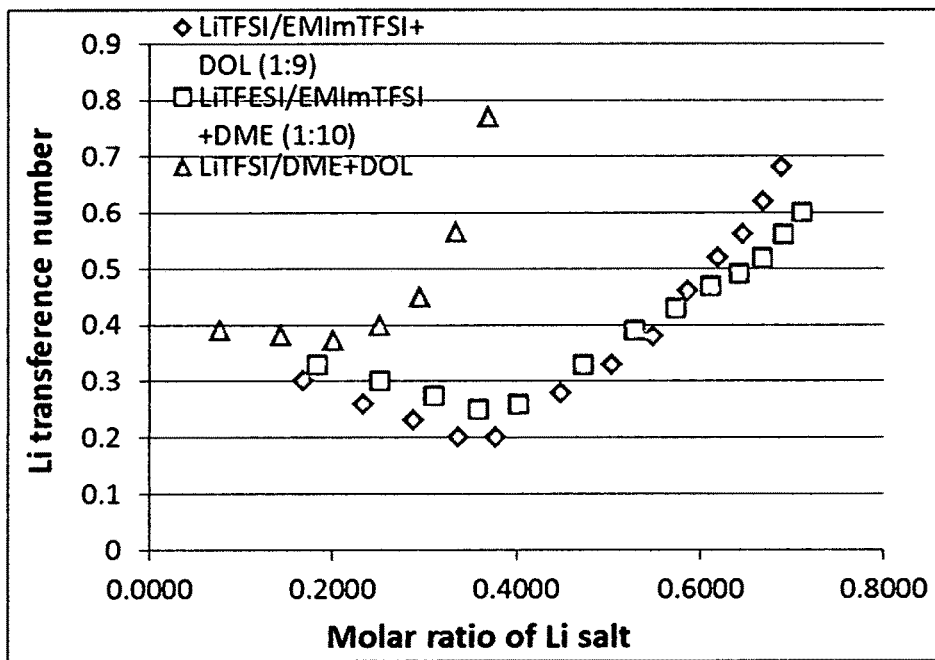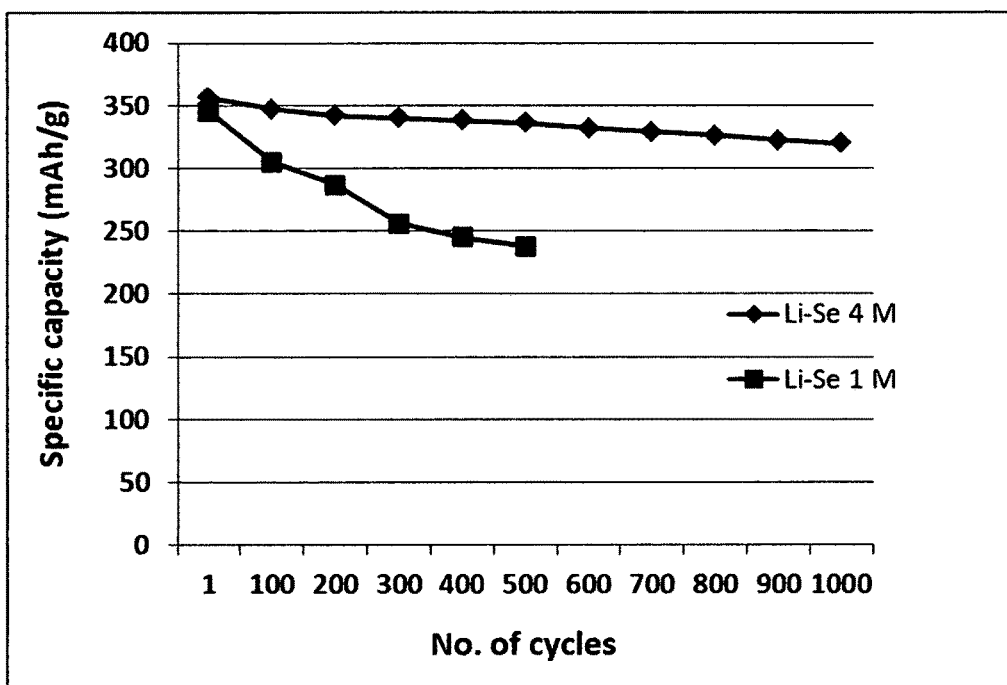
FIG. 5
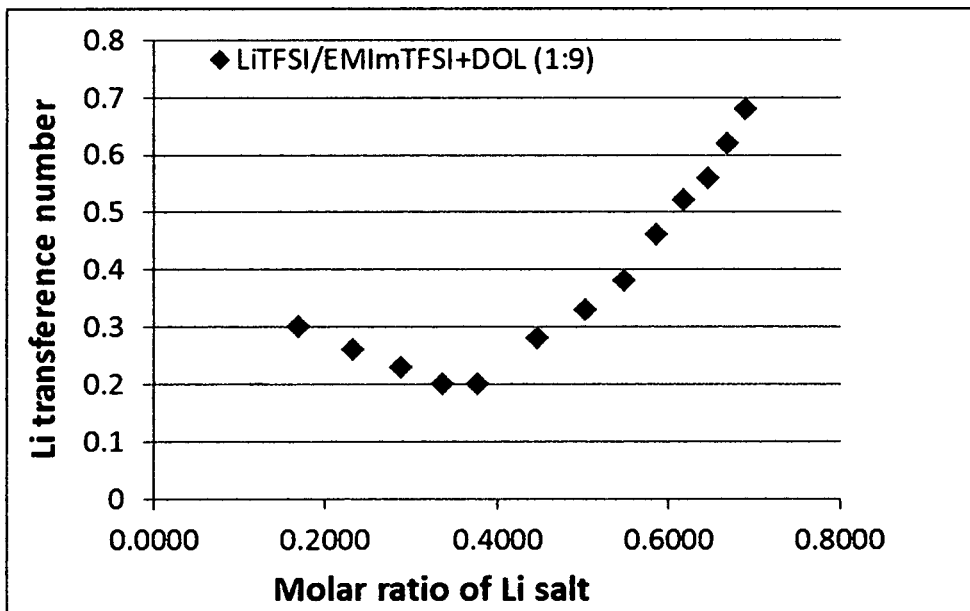
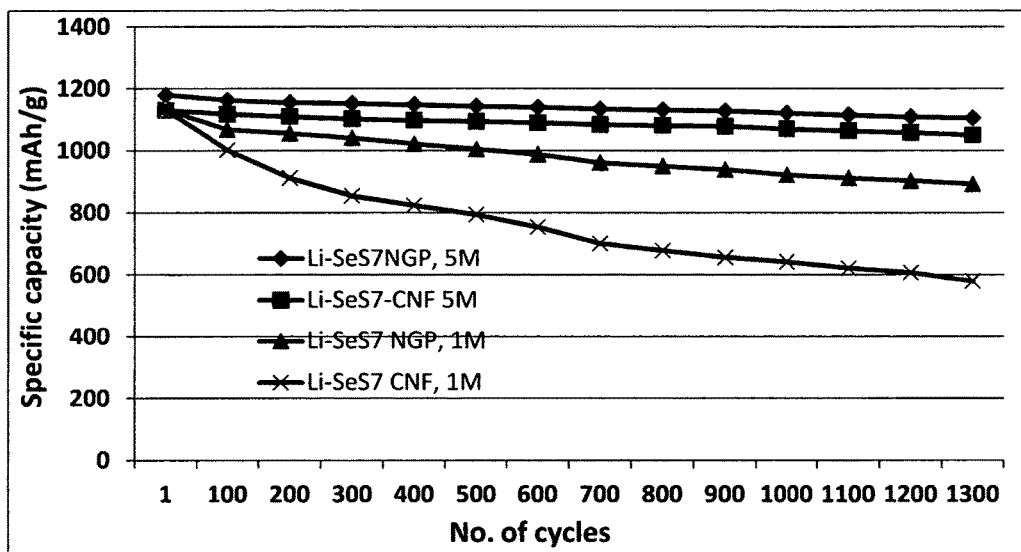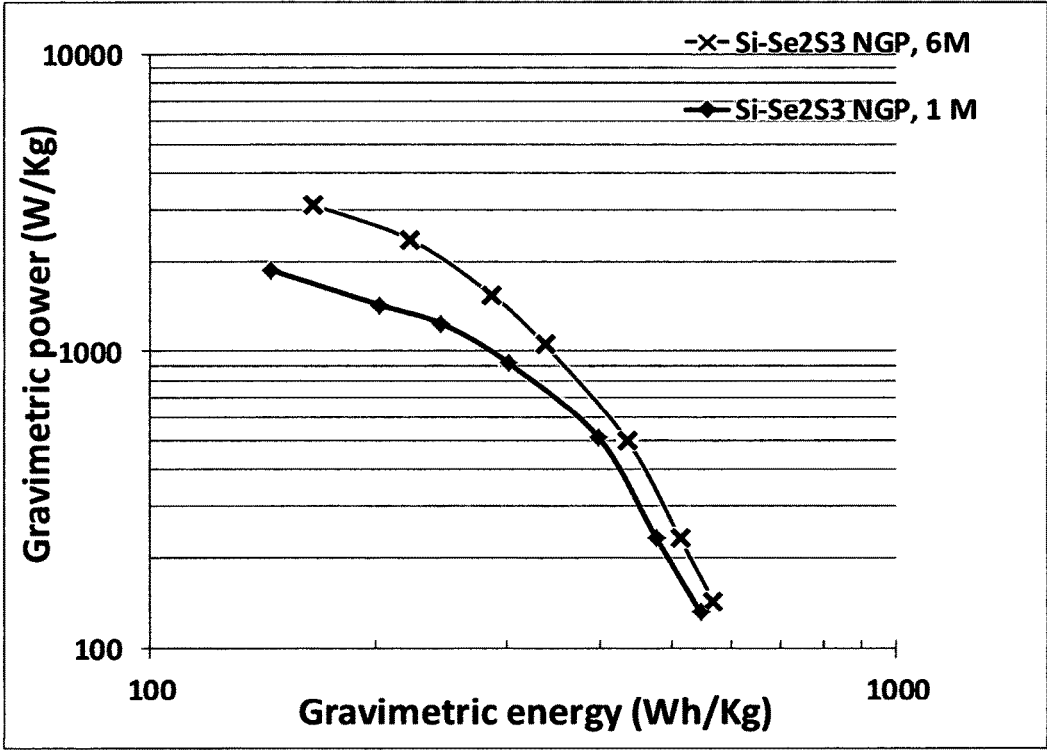**FIG. 6**

FIG. 7

FIG. 8

FIG. 9

FIG. 10

FIG. 11

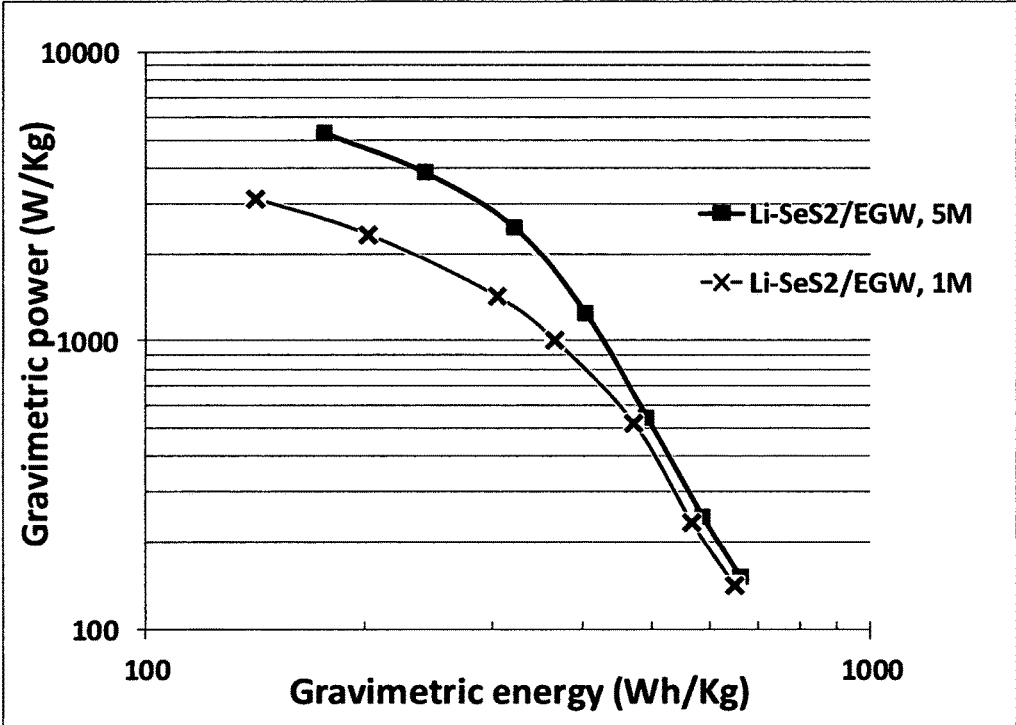FIG. 12

LITHIUM-SELENIUM SECONDARY BATTERIES HAVING NON-FLAMMABLE ELECTROLYTE

FIELD OF THE INVENTION

The present invention provides a secondary or rechargeable lithium-selenium battery containing a non-flammable electrolyte composition.

BACKGROUND

Rechargeable lithium-ion (Li-ion), lithium metal, lithium-sulfur, and Li metal-air batteries are considered promising power sources for electric vehicle (EV), hybrid electric vehicle (HEV), and portable electronic devices, such as lap-top computers and mobile phones. Lithium as a metal element has the highest lithium storage capacity (3,861 mAh/g) compared to any other metal or metal-intercalated compound as an anode active material (except $Li_{4.4}Si$, which has a specific capacity of 4,200 mAh/g). Hence, in general, Li metal batteries (having a lithium metal anode) have a significantly higher energy density than conventional lithium-ion batteries (having a graphite anode).

Historically, rechargeable lithium metal batteries were produced using non-lithiated compounds having relatively high specific capacities, such as TiS_2, MoS_2, MnO_2, CoO_2, and V_2O_5, as the cathode active materials, which were coupled with a lithium metal anode. When the battery was discharged, lithium ions were transferred from the lithium metal anode to the cathode through the electrolyte and the cathode became lithiated. Unfortunately, upon repeated charges and discharges, the lithium metal resulted in the formation of dendrites at the anode that ultimately caused internal shorting, thermal runaway, and explosion. As a result of a series of accidents associated with this problem, the production of these types of secondary batteries was stopped in the early 1990's giving ways to lithium-ion batteries.

Even now, cycling stability and safety concerns remain the primary factors preventing the further commercialization of Li metal batteries (e.g. Lithium-sulfur and Lithium-transition metal oxide cells) for EV, HEV, and microelectronic device applications. Again, cycling stability and safety issues of lithium metal rechargeable batteries are primarily related to the high tendency for Li metal to form dendrite structures during repeated charge-discharge cycles or overcharges, leading to internal electrical shorting and thermal runaway. This thermal runaway or even explosion is caused by the organic liquid solvents used in the electrolyte (e.g. carbonate and ether families of solvents), which are unfortunately highly volatile and flammable.

Many attempts have been made to address the dendrite and thermal runaway issues. However, despite these earlier efforts, no rechargeable Li metal batteries have succeeded in the market place. This is likely due to the notion that these prior art approaches still have major deficiencies. For instance, in several cases, the anode or electrolyte structures designed for prevention of dendrites are too complex. In others, the materials are too costly or the processes for making these materials are too laborious or difficult. Most critically, in most of the lithium metal cells and lithium-ion cells, the electrolyte solvents are flammable. An urgent need exists for a simpler, more cost-effective, and easier to implement approach to preventing Li metal dendrite-induced internal short circuit and thermal runaway problems in Li metal batteries.

Parallel to these efforts and prompted by the aforementioned concerns over the safety of earlier lithium metal secondary batteries led to the development of lithium-ion secondary batteries, in which pure lithium metal sheet or film was replaced by carbonaceous materials (e.g. natural graphite particles) as the anode active material. The carbonaceous material absorbs lithium (through intercalation of lithium ions or atoms between graphene planes, for instance) and desorbs lithium ions during the re-charge and discharge phases, respectively, of the lithium-ion battery operation. The carbonaceous material may comprise primarily graphite that can be intercalated with lithium and the resulting graphite intercalation compound may be expressed as Li_xC_6, where x is typically less than 1.

Although lithium-ion (Li-ion) batteries are promising energy storage devices for electric drive vehicles, state-of-the-art Li-ion batteries have yet to meet the cost, safety, and performance targets. Li-ion cells typically use a lithium transition-metal oxide or phosphate as a positive electrode (cathode) that de/re-intercalates Li^+ at a high potential with respect to the carbon negative electrode (anode). The specific capacity of lithium transition-metal oxide or phosphate based cathode active material is typically in the range of 140-170 mAh/g. As a result, the specific energy of commercially available Li-ion cells is typically in the range of 120-220 Wh/kg, most typically 150-200 Wh/kg. These specific energy values are two to three times lower than what would be required for battery-powered electric vehicles to be widely accepted.

Furthermore, the same flammable solvents previously used for lithium metal secondary batteries are also used in most of the lithium-ion batteries. Despite the notion that there is significantly reduced propensity of forming dendrites in a lithium-ion cell (relative to a lithium metal cell), the lithium-ion cell has its own intrinsic safety issue. For instance, the transition metal elements in the lithium metal oxide cathode are highly active catalysts that can promote and accelerate the decomposition of organic solvents, causing thermal runaway or explosion initiation to occur at a relatively low electrolyte temperature (e.g. <200° C., as opposed to normally 400° C. without the catalytic effect).

Ionic liquids (ILs) are a new class of purely ionic, salt-like materials that are liquid at unusually low temperatures. The official definition of ILs uses the boiling point of water as a point of reference: "Ionic liquids are ionic compounds which are liquid below 100° C.". A particularly useful and scientifically interesting class of ILs is the room temperature ionic liquid (RTIL), which refers to the salts that are liquid at room temperature or below. RTILs are also referred to as organic liquid salts or organic molten salts. An accepted definition of an RTIL is any salt that has a melting temperature lower than ambient temperature.

Although ILs were suggested as a potential electrolyte for rechargeable lithium batteries due to their non-flammability, conventional ionic liquid compositions have not exhibited satisfactory performance when used as an electrolyte likely due to several inherent drawbacks: (a) ILs have relatively high viscosity at room or lower temperatures; thus being considered as not amenable to lithium ion transport; (b) For Li—S cell uses, ILs are capable of dissolving lithium polysulfides at the cathode and allowing the dissolved species to migrate to the anode (i.e., the shuttle effect remains severe); and (c) For lithium metal secondary cells, most of the ILs strongly react with lithium metal at the anode, continuing to consume Li and deplete the electrolyte itself during repeated charges and discharges. These factors lead to relatively poor specific capacity (particularly under

high current or high charge/discharge rate conditions, hence lower power density), low specific energy density, rapid capacity decay and poor cycle life. Furthermore, ILs remain extremely expensive. Consequently, as of today, no commercially available lithium battery makes use of an ionic liquid as the primary electrolyte component.

With the rapid development of hybrid (HEV), plug-in hybrid electric vehicles (HEV), and all-battery electric vehicles (EV), there is an urgent need for anode and cathode materials and electrolytes that provide a rechargeable battery with a significantly higher specific energy, higher energy density, higher rate capability, long cycle life, and safety. One of the most promising energy storage devices is the lithium-sulfur (Li—S) cell since the theoretical capacity of Li is 3,861 mAh/g and that of S is 1,675 mAh/g. In its simplest form, a Li—S cell consists of elemental sulfur as the positive electrode and lithium as the negative electrode. The lithium-sulfur cell operates with a redox couple, described by the reaction $S_8+16Li \leftrightarrow 8Li_2S$ that lies near 2.2 V with respect to Li^-/Li°. This electrochemical potential is approximately ⅔ of that exhibited by conventional positive electrodes. However, this shortcoming is offset by the very high theoretical capacities of both Li and S. Thus, compared with conventional intercalation-based Li-ion batteries, Li—S cells have the opportunity to provide a significantly higher energy density (a product of capacity and voltage). Values can approach 2,500 Wh/kg or 2,800 Wh/l based on the combined Li and S weight or volume (not based on the total cell weight or volume), respectively, assuming complete reaction to Li_2S. With a proper cell design, a cell-level specific energy of 1,200 Wh/kg (of cell weight) and cell-level energy density of 1,400 Wh/l (of cell volume) should be achievable. However, the current Li-sulfur products of industry leaders in sulfur cathode technology have a maximum cell specific energy of 200-400 Wh/kg (based on the total cell weight), far less than what could be obtained in real practice.

In summary, despite its considerable advantages, the rechargeable lithium metal cell in general and the Li—S cell in particular are plagued with several major technical problems that have hindered its widespread commercialization:

(1) Conventional lithium metal secondary cells (e.g., rechargeable Li metal cells, Li—S cells, and Li-Air cells) still have dendrite formation and related internal shorting and thermal runaway issues. Also, conventional Li-ion cells still make use of significant amounts of flammable liquids (e.g. propylene carbonate, ethylene carbonate, and 1,3-dioxolane) as the primary electrolyte solvent, risking danger of explosion;

(2) The Li—S cell tends to exhibit significant capacity fade during discharge-charge cycling. This is mainly due to the high solubility of the lithium polysulfide anions formed as reaction intermediates during both discharge and charge processes in the polar organic solvents used in electrolytes. During cycling, the lithium polysulfide anions can migrate through the separator and electrolyte to the Li negative electrode whereupon they are reduced to solid precipitates (Li_2S_2 and/or Li_2S), causing active mass loss. In addition, the solid product that precipitates on the surface of the positive electrode during discharge can become electrochemically irreversible, which also contributes to active mass loss.

(3) More generally speaking, a significant drawback with cells containing cathodes comprising elemental sulfur, organosulfur and carbon-sulfur materials relates to the dissolution and excessive out-diffusion of soluble sulfides, polysulfides, organo-sulfides, carbon-sulfides and/

or carbon-polysulfides (hereinafter referred to as anionic reduction products) from the cathode into the rest of the cell. This phenomenon is commonly referred to as the Shuttle Effect. This process leads to several problems: high self-discharge rates, loss of cathode capacity, corrosion of current collectors and electrical leads leading to loss of electrical contact to active cell components, fouling of the anode surface giving rise to malfunction of the anode, and clogging of the pores in the cell membrane separator which leads to loss of ion transport and large increases in internal resistance in the cell.

(4) Sulfur is an extremely insulating material with an electrical conductivity as low as 5×10^{-30} S/cm. Hence, the cathode requires the use of a large amount (30-50% by weight) of a conductive additive (e.g. carbon black), which is not a cathode active material (not capable of storing Li). This significantly reduces the cathode specific capacity (based on total cathode composite weight) and specific energy of the cell.

(5) A recently developed lithium metal cell (Li—Se) suffers from the same types of problems associated with Li—S cells [e.g. Chao Luo, et al. "Selenium@Mesoporous Carbon Composite with Superior Lithium and Sodium Storage Capacity," *ACS Nano*, Article ASAP, DOI: 10.1021/nn403108w].

In response to these challenges, new electrolytes, protective films for the lithium anode, and solid-state electrolytes have been developed. Some interesting cathode developments have been reported recently to contain lithium polysulfides; but, their performance still fall short of what is required for practical applications. Despite the various approaches proposed for the fabrication of high energy density rechargeable cells containing elemental sulfur, organo-sulfur and carbon-sulfur cathode materials, or derivatives and combinations thereof, there remains a strong need for a safer and higher-performing rechargeable lithium metal cell.

Responsive to this need, a general object of the present invention is to provide an electrolyte system for a rechargeable lithium-selenium cell that exhibits a high energy density, high power density, long cycle life, and no danger of explosion due to the use of a safer, non-flammable, quasi-solid electrolyte. The invention also provides a rechargeable lithium-selenium cell containing such a safe electrolyte system. This lithium-selenium cell includes the lithium metal secondary cell (e.g. Li—Se or Li—Se_xS_y cell, where x/y ratio is from 0.01 to 100, using lithium metal as the anode and Se or Se_xS_y as the cathode active material) and the lithium-ion selenium cell (e.g. prelithiated Si—Se cell, prelithiated Si—Se_xS_y cells, prelithiated Sn—Se cell, and prelithiated Sn—Se_xS_y cells, where high-capacity anode active materials, such as Si and Sn, are lithiated to serve as the anode active material).

A specific object of the present invention is to provide a rechargeable lithium-selenium battery that exhibits an exceptionally high specific energy or high energy density and a high level of safety. One specific technical goal of the present invention is to provide a safe lithium-selenium cell having a long cycle life and a cell specific energy greater than 400 Wh/Kg, preferably greater than 500 Wh/Kg, and more preferably greater than 600 Wh/Kg (all based on the total cell weight).

Another specific object of the present invention is to provide a safe lithium-selenium cell that exhibits a high specific capacity (e.g., higher than 800 mAh/g based on the Se_xS_y weight, or higher than 600 mAh/g based on the cathode composite weight, including Se_xS_y, conducting

additive and conductive substrate, and binder weights combined, but excluding the weight of cathode current collector). The specific capacity is preferably higher than 1,000 mAh/g based on the Se_xS_y weight alone or higher than 800 mAh/g based on the cathode composite weight. This must be accompanied by a high specific energy, good resistance to dendrite formation, good resistance to thermal runaway, no possibility of an explosion, and a long and stable cycle life.

It may be noted that in most of the open literature reports (scientific papers) on Li—S cells, scientists choose to express the cathode specific capacity based on the sulfur weight or lithium polysulfide weight alone (not on the total cathode composite weight), but unfortunately a large proportion of non-active materials (those not capable of storing lithium, such as conductive additive and binder) is typically used in their Li—S cells. Similarly, for lithium-selenium cells, scientists also tend to report the cathode specific capacity based on the Se_xS_y weight only. For practical usage purposes, it is more meaningful to use the cathode composite weight-based capacity value.

A specific object of the present invention is to provide a rechargeable lithium-selenium cell based on rational materials and battery designs that overcome or significantly reduce the following issues commonly associated with conventional Li—S and Li—Se cells: (a) dendrite formation (internal shorting); (b) extremely low electric and ionic conductivities of sulfur, requiring large proportion (typically 30-55%) of non-active conductive fillers and having significant proportion of non-accessible or non-reachable sulfur or lithium polysulfides); (c) dissolution of lithium polysulfide in electrolyte and migration of dissolved lithium polysulfides from the cathode to the anode (which irreversibly react with lithium at the anode), resulting in active material loss and capacity decay (the shuttle effect); and (d) short cycle life.

Another object of the present invention is to provide a simple, cost-effective, and easy-to-implement approach to preventing potential Li metal dendrite-induced internal short circuit and thermal runaway problems in various Li metal and Li-ion batteries.

SUMMARY OF THE INVENTION

As a first embodiment, the present invention provides a rechargeable lithium-selenium cell comprising a cathode having a cathode active material selected from Se or Se_xS_y (x/y ratio=0.01 to 100), an anode having an anode active material, a porous separator electronically separating the anode and the cathode, a non-flammable quasi-solid electrolyte in contact with the cathode and the anode, wherein the electrolyte contains a lithium salt dissolved in a first organic liquid solvent with a lithium salt concentration sufficiently high so that the electrolyte exhibits a vapor pressure less than 0.01 kPa when measured at 20° C., a vapor pressure less than 60% of the vapor pressure of the first organic solvent alone, a flash point at least 20 degrees Celsius higher than a flash point of the first organic liquid solvent alone, a flash point higher than 150° C., or no flash point.

In a preferred embodiment, the cathode active material contains Se (no S), plus an optional conductive additive or conductive support, and an optional resin binder. In this case, the lithium-selenium cell is a Li—Se cell. Another preferred version of the rechargeable lithium-selenium cell is referred to as a Li—Se/S cell containing a cathode active material Se_xS_y, wherein the x/y ratio is from 0.05 to 20. We have found that Se and S can be mixed to form an alloy at

any ratio. Most preferably, Se_xS_y is selected from Se_5S, Se_5S_2, Se_5S_4, SeS, Se_3S_5, SeS_2, SeS_7, or SeS_z, where z is from 7 to 20.

We have surprisingly discovered that the flammability of any organic solvent can be effectively suppressed provided that a sufficiently high amount of a lithium salt is added to and dissolved in this organic solvent to form a solid-like or quasi-solid electrolyte. In general, such a quasi-solid electrolyte exhibits a vapor pressure less than 0.01 kPa (when measured at 20° C.) and less than 0.1 kPa (when measured at 100° C.). In many cases, the vapor molecules are practically too few to be detected. The high solubility of the lithium salt in an otherwise highly volatile solvent has effectively prevented the flammable gas molecules from initiating a flame even at an extremely high temperature (e.g. using a torch). The flash point of the quasi-solid electrolyte is typically higher than the flash point of the neat organic solvent alone by at least 20 degrees (often by least 50 degrees or even 100 degrees centigrade). In most of the cases, either the flash point is higher than 150° C. or no flash point can be detected. The electrolyte just would not catch on fire or get ignited. Any accidentally initiated flame does not sustain for longer than a few seconds. This is a highly significant discovery, considering the notion that fire and explosion concern has been a major impediment to widespread acceptance of battery-powered electric vehicles. This new technology could potentially reshape the landscape of EV industry.

Another surprising element of the present invention is the notion that we are able to dissolve a high concentration of a lithium salt in an organic solvent to form an electrolyte suitable for use in a rechargeable lithium battery. This concentration is typically greater than a lithium salt molecular ratio >0.2, more typically >0.3, can be >0.4, 0.5, 0.6, and even >0.7. In a more easily understood but scientifically not accurate manner, the concentration is typically greater than 2.5 M (mole/liter), more typically and preferably greater than 3.5 M, still more typically and preferably greater than 5 M, further more preferably greater than 7 M, and most preferably greater than 10 M. Such a high concentration of lithium salt in a solvent has not been generally considered possible. Indeed, in general, it has not been possible to achieve such a high concentration of lithium salt in an organic solvent used in a battery electrolyte. After an extensive and in-depth study, we came to further discover that the apparent solubility of a lithium salt could be significantly increased if(a) a highly volatile co-solvent is used to increase the amount of lithium salt dissolved in the solvent mixture first and then (b) this volatile co-solvent is partially or totally removed once the dissolution procedure is completed. Quite unexpectedly, the removal of this co-solvent typically did not lead to precipitation or crystallization of the lithium salt out of the solution even though the solution would have been in a highly supersaturated state. This novel and unique approach appears to have produced a material state wherein most of the solvent molecules are retained or captured by lithium salt ions that are not volatile. Hence, very few solvent molecules are able to escape into the vapor phase. Consequently, very few volatile gas molecules can be present to initiate or sustain a flame. This has not been suggested as technically possible or viable in any previous report.

It may be noted that a good scientist in the field of chemistry or materials science would not even consider such a high salt concentration desirable since a high salt concentration would make the electrolyte behave like a solid with an extremely high viscosity and, hence, this electrolyte

would not be amenable to fast diffusion of lithium ions therein. Consequently, the scientist would tend to expect that a lithium battery containing such a solid-like electrolyte would not and could not exhibit a high capacity at a high charge-discharge rate or under a high current density condition (i.e. the battery should have a poor rate capability). Contrary to these expectations, all the lithium-selenium cells containing such a quasi-solid electrolyte deliver surprisingly high energy density and high power density for a long cycle life. The quasi-solid electrolytes as herein disclosed are conducive to facile lithium ion transport. This surprising observation is manifested by a high lithium ion transference number (TN), to be further explained in a later section of this specification. We have found that the quasi-solid electrolytes provide a TN greater than 0.4 (typically in the range of 0.4-0.8), in contrast to the typical values of 0.1-0.2 in all lower concentration electrolytes (e.g. <2.0 M) used in all current Li-ion and Li—S cells. The rechargeable lithium-selenium cell preferably contains a quasi-solid electrolyte having a lithium ion transference number greater than 0.4, preferably and typically greater than 0.6, and most preferably and typically greater than 0.7.

In an embodiment, the first organic liquid solvent may be selected from the group consisting of 1,3-dioxolane (DOL), 1,2-dimethoxyethane (DME), tetraethylene glycol dimethylether (TEGDME), poly(ethylene glycol) dimethyl ether (PEGDME), diethylene glycol dibutyl ether (DEGDBE), 2-ethoxyethyl ether (EEE), sulfone, sulfolane, ethylene carbonate (EC), dimethyl carbonate (DMC), methylethyl carbonate (MEC), diethyl carbonate (DEC), ethyl propionate, methyl propionate, propylene carbonate (PC), gamma-butyrolactone (γ-BL), acetonitrile (AN), ethyl acetate (EA), propyl formate (PF), methyl formate (MF), toluene, xylene, methyl acetate (MA), fluoroethylene carbonate (FEC), vinylene carbonate (VC), allyl ethyl carbonate (AEC), a hydrofluoroether (e.g. methyl perfluorobutyl ether, MFE, or ethyl perfluorobutyl ether, EFE), an ionic liquid solvent, and combinations thereof.

The lithium salt may be selected from lithium perchlorate ($LiClO_4$), lithium hexafluoro-phosphate ($LiPF_6$), lithium borofluoride ($LiBF_4$), lithium hexafluoroarsenide ($LiAsF_6$), lithium trifluoro-metasulfonate ($LiCF_3SO_3$), bis-trifluoromethyl sulfonylimide lithium ($LiN(CF_3SO_2)_2$), lithium bis (oxalato)borate (LiBOB), lithium oxalyldifluoroborate ($LiBF_2C_2O_4$), lithium oxalyldifluoroborate ($LiBF_2C_2O_4$), lithium nitrate ($LiNO_3$), Li-Fluoroalkyl-Phosphates ($LiPF_3$ ($CF_2CF_3)_3$), lithium bisperfluoro-ethysulfonylimide (Li-BETI), lithium bis(trifluoromethanesulphonyl)imide, lithium bis(fluorosulphonyl)imide, lithium trifluoromethanesulfonimide (LiTFSI), an ionic liquid lithium salt, or a combination thereof.

In a preferred embodiment, the lithium salt concentration, when expressed in terms of molecular ratio, is greater than 0.2 (preferably and typically >0.3, more preferably and typically >0.4, and most preferably and typically >0.5). This lithium salt concentration, when expressed in terms of mole/liter, is typically significantly greater than 3.5 M, more preferably greater than 5 M, further more preferably greater than 6 M, still more preferably greater than 7 M, and most preferably greater than 8 M. In some electrolytes, lithium salt concentrations are higher than 10 M. These are extremely surprising, indeed.

In an embodiment, the electrolyte further contains an ionic liquid solvent and a first organic liquid solvent-to-ionic liquid solvent ratio is greater than 1/1, preferably greater than 3/1. The ionic liquid solvent is preferably selected from a room temperature ionic liquid having a cation selected

from tetraalkylammonium, di-, tri-, or tetra-alkylimidazolium, alkylpyridinium, dialkyl-pyrrolidinium, dialkylpiperidinium, tetraalkylphosphonium, trialkylsulfonium, or a combination thereof. The room temperature ionic liquid preferably has an anion selected from BF_4^-, $B(CN)_4^-$, $CH_3BF_3^-$, $CH_2CHBF_3^-$, $CF_3BF_3^-$, $C_2F_5BF_3^-$, $n-C_3F_7BF_3^-$, $n-C_4F_9BF_3^-$, PF_6^-, $CF_3CO_2^-$, $CF_3SO_3^-$, $N(SO_2CF_3)_2^-$, $N(COCF_3)(SO_2CF_3)^-$, $N(SO_2F)_2^-$, $N(CN)_2^-$, $C(CN)_3^-$, SCN^-, $SeCN^-$, $CuCl_2^-$, $AlCl_4^-$, $F(HF)_{2.3}^-$, or a combination thereof.

In any of the aforementioned rechargeable lithium-selenium cell, the anode may contain an anode active material selected from lithium metal, a lithium metal alloy, a mixture of lithium metal or lithium alloy with a lithium intercalation compound, a lithiated compound, lithiated titanium dioxide, lithium titanate, lithium manganate, a lithium transition metal oxide, $Li_4Ti_5O_{12}$, or a combination thereof.

Alternatively, the anode may contain an anode active material selected from the group consisting of: (a) silicon (Si), germanium (Ge), tin (Sn), lead (Pb), antimony (Sb), bismuth (Bi), zinc (Zn), aluminum (Al), nickel (Ni), cobalt (Co), manganese (Mn), titanium (Ti), iron (Fe), and cadmium (Cd), and lithiated versions thereof; (b) alloys or intermetallic compounds of Si, Ge, Sn, Pb, Sb, Bi, Zn, Al, or Cd with other elements, and lithiated versions thereof, wherein said alloys or compounds are stoichiometric or non-stoichiometric; (c) oxides, carbides, nitrides, sulfides, phosphides, selenides, and tellurides of Si, Ge, Sn, Pb, Sb, Bi, Zn, Al, Fe, Ni, Co, Ti, Mn, or Cd, and their mixtures or composites, and lithiated versions thereof; (d) salts and hydroxides of Sn and lithiated versions thereof; (e) carbon or graphite materials and prelithiated versions thereof; and combinations thereof. The carbon or graphite materials may be selected from the group consisting of natural graphite particles, synthetic graphite particles, needle cokes, electrospun nano fibers, vapor-grown carbon or graphite nano fibers, carbon or graphite whiskers, carbon nano-tubes, carbon nanowires, sheets and platelets of pristine graphene, graphene oxide, reduced graphene oxide, doped graphene or graphene oxide, and chemically functionalized graphene, and combinations thereof.

The rechargeable lithium-selenium cell may further comprise a cathode current collector selected from aluminum foil, carbon- or graphene-coated aluminum foil, stainless steel foil or web, carbon- or graphene-coated steel foil or web, carbon or graphite paper, carbon or graphite fiber fabric, flexible graphite foil, graphene paper or film, or a combination thereof. A web means a screen-like structure or a metal foam, preferably having interconnected pores or through-thickness apertures. The lithium-selenium cell may further comprise an anode current collector selected from copper foil or web, carbon- or graphene-coated copper foil or web, stainless steel foil or web, carbon- or graphene-coated steel foil or web, titanium foil or web, carbon- or graphene-coated titanium foil or web carbon or graphite paper, carbon or graphite fiber fabric, flexible graphite foil, graphene paper or film, or a combination thereof.

Another embodiment of the present invention is a rechargeable lithium-selenium cell comprising a cathode having a cathode active material selected from Se or Se_xS_y, (x/y ratio=0.01 to 100), an anode having an anode active material, a porous separator electronically separating the anode and the cathode, a non-flammable quasi-solid electrolyte in contact with the cathode and the anode, wherein the cathode active material is supported by a network of conductive nano filaments selected from carbon nano-tubes, carbon nano-fibers, graphene sheets, exfoliated graphite

flakes, carbon black, or a combination thereof and the electrolyte contains a lithium salt dissolved in a first organic liquid solvent with a lithium salt concentration higher than 1.5 M (preferably >2.5 M and more preferably >3.5 M) so that the electrolyte exhibits a vapor pressure less than 0.02 kPa when measured at 20° C., a vapor pressure less than 60% of the vapor pressure of the first organic solvent alone, a flash point at least 20 degrees Celsius higher than a flash point of said first organic liquid solvent alone, a flash point higher than 150° C., or no flash point can be detected.

The presently invented lithium-selenium cell provides a reversible specific capacity of typically no less than 800 mAh per gram based on the total weight of Se or Se_xS_y, and the conductive support or additive combined. More typically and preferably, the reversible specific capacity is no less than 1,000 mAh per gram and often exceeds 1,200 mAh per gram. The high specific capacity of the presently invented cathode, when in combination with a lithium anode, leads to a cell specific energy of no less than 600 Wh/Kg based on the total cell weight including anode, cathode, electrolyte, separator, and current collector weights combined. In many cases, the cell specific energy is higher than 800 Wh/Kg and, in some examples, exceeds 1,000 Wh/kg.

These and other advantages and features of the present invention will become more transparent with the description of the following best mode practice and illustrative examples.

BRIEF DESCRIPTION OF THE DRAWINGS

FIG. 1 Vapor pressure ratio data (p_s/p=vapor pressure of solution/vapor pressure of solvent alone) as a function of the lithium salt molecular ratio x (LiTFSI/DOL), along with the theoretical predictions based on the classic Raoult's Law.

FIG. 2 Vapor pressure ratio data (p_s/p=vapor pressure of solution/vapor pressure of solvent alone) as a function of the lithium salt molecular ratio x (LiTFSI/DME), along with the theoretical predictions based on classic Raoult's Law.

FIG. 3 Vapor pressure ratio data (p_s/p=vapor pressure of solution/vapor pressure of solvent alone) as a function of the lithium salt molecular ratio x (LiPF$_6$/DOL), along with the theoretical predictions based on classic Raoult's Law.

FIG. 4 Vapor pressure ratio data (p_s/p=vapor pressure of solution/vapor pressure of solvent alone) as a function of the lithium salt molecular ratio x (LiTFSI/DOL, LiTFSI/DME, LiPF$_6$/DOL), along with the theoretical predictions based on classic Raoult's Law.

FIG. 5 The Li^+ ion transference numbers of electrolytes (e.g. LiTFSI salt/(DOL+DME) solvents) in relation to the lithium salt molecular ratio x.

FIG. 6 The Li^+ ion transference numbers of electrolytes (e.g. LiTFSI salt/(EMImTFSI+DOL) solvents) in relation to the lithium salt molecular ratio x.

FIG. 7 The Li^+ ion transference numbers of electrolytes (e.g. LiTFSI salt/(EMImTFSI+DME) solvents) in relation to the lithium salt molecular ratio x.

FIG. 8 The Li^+ ion transference numbers in various electrolytes (as in FIG. 6-8) in relation to the lithium salt molecular ratio x.

FIG. 9 The cycling performance (discharge specific capacity) of a Li metal-selenium (Li—Se) cell containing a low-concentration electrolyte (1 M of LiTFSI salt in (DOL+DME) solvent) and that of a corresponding cell containing a quasi-solid electrolyte (4 M).

FIG. 10 The discharge specific capacity of 4 Li—SeS$_7$ cells: two containing an organic liquid solvent-based quasi-solid electrolyte (5 M of LiClO$_4$ in DOL+PC) and the other

two containing a conventional electrolyte (1 M). Each cell has either a graphene (NGP) nanostructure or a carbon nano-fiber (CNF) nanostructure to support the cathode active material (SeS$_7$ alloy).

FIG. 11 Ragone plots (cell power density vs. cell energy density) of two Li-ion Se/S cells each having a prelithiated Si nano particle anode and a graphene-supported Se$_2$S$_3$ alloy cathode, but with the lithium salt concentrations being 1 M and 6M, respectively.

FIG. 12 The energy density and power density data of two Li—SeS$_2$ cells having an exfoliated graphite worm-supported SeS$_2$ alloy as the cathode. One cell has a conventional low-concentration electrolyte (1 M) and the other a quasi-solid electrolyte (5 M).

DETAILED DESCRIPTION OF PREFERRED EMBODIMENTS

The present invention provides a safe and high-performing rechargeable lithium-selenium battery, which can be the lithium metal-selenium cell (i.e. Li—Se having lithium metal as an anode active material and sulfur-free Se as the cathode active material), a lithium-ion selenium cell (e.g. a lithium intercalation compound, such as Si or Sn, as an anode active material and sulfur-free Se as the cathode active material), a lithium metal-selenium/sulfur cell (i.e. Li—Se/S having lithium metal as an anode active material and Se$_x$S$_y$, a mixture or alloy of Se and S, as the cathode active material), or lithium-ion selenium/sulfur cell (e.g. a lithium intercalation compound, such as Si or Sn, as an anode active material and Se$_x$S$_y$ as the cathode active material), where the ratio x/y is from 0.01 to 100. A high degree of safety is imparted to this battery by a novel and unique electrolyte that is essentially non-flammable and would not initiate a fire or sustain a fire and, hence, would not pose explosion danger. This invention has solved the very most critical issue that has plagued the lithium-metal and lithium-ion industries for more than two decades.

The inventive cell comprises a cathode having a cathode active material (Se or Se$_x$S$_y$) and an optional conductive cathode-supporting structure, an anode having an anode active material and/or a conductive supporting nano-structure, a separator electronically separating the anode and the cathode, an organic solvent-based highly concentrated electrolyte in contact with the cathode active material and the anode active material, wherein the electrolyte contains a lithium salt dissolved in a first organic liquid solvent with a lithium salt molecular ratio sufficiently high so that the electrolyte exhibits a vapor pressure less than 0.01 kPa or less than 0.6 (60%) of the vapor pressure of the solvent alone (when measured at 20° C.), a flash point at least 20 degrees Celsius higher than a flash point of the first organic liquid solvent alone (when no lithium salt is present), a flash point higher than 150° C., or no detectable flash point at all.

Most surprising and of tremendous scientific and technological significance is our discovery that the flammability of any volatile organic solvent can be effectively suppressed provided that a sufficiently high amount of a lithium salt is added to and dissolved in this organic solvent to form a solid-like or quasi-solid electrolyte. In general, such a quasi-solid electrolyte exhibits a vapor pressure less than 0.01 kPa and often less than 0.001 kPa (when measured at 20° C.) and less than 0.1 kPa and often less than 0.01 kPa (when measured at 100° C.). (The vapor pressures of the corresponding neat solvent, without any lithium salt dissolved therein, are typically significantly higher.) In many cases, the vapor molecules are practically too few to be detected.

A highly significant observation is that the high solubility of the lithium salt in an otherwise highly volatile solvent (a large molecular ratio or molar fraction of lithium salt, typically >0.2, more typically >0.3, and often >0.4 or even >0.5) has dramatically curtailed the amount of volatile solvent molecules that can escape into the vapor phase in a thermodynamic equilibrium condition. In many cases, this has effectively prevented the flammable gas molecules from initiating a flame even at an extremely high temperature (e.g. using a torch). The flash point of the quasi-solid electrolyte is typically at least 20 degrees (often >50 degrees) higher than the flash point of the neat organic solvent alone. In most of the cases, either the flash point is higher than 150° C. or no flash point can be detected. The electrolyte just would not catch on fire. Furthermore, any accidentally initiated flame does not sustain for longer than a few seconds. This is a highly significant discovery, considering the notion that fire and explosion concern has been a major impediment to widespread acceptance of battery-powered electric vehicles. This new technology could significantly impact the emergence of a vibrant EV industry.

From the perspective of fundamental chemistry principles, addition of solute molecules to a liquid elevates the boiling temperature of the liquid and reduces its vapor pressure and freezing temperature. These phenomena, as well as osmosis, depend only on the solute concentration and not on its type, and are called colligative properties of solutions. The original Raoult's law provides the relationship between the ratio of the vapor pressure (p_s) of a solution to the vapor pressure (p) of the pure liquid and the molar fraction of the solute (x):

$$p_s/p=e^{-x} \qquad\qquad \text{Eq. (1a)}$$

For a dilute solution, $x\ll1$ and, hence, $e^{-x}\approx1-x$. Thus, for the special cases of low solute molar fractions, one obtains a more familiar form of Raoult's law:

$$p_s/p=1-x \qquad\qquad \text{Eq. (1b)}$$

In order to determine if the classic Raoult's law can be used to predict the vapor pressures of highly concentrated electrolytes, we proceeded to investigate a broad array of lithium salt/organic solvent combinations. Some of the examples of our research results are summarized in FIG. 1 FIG. 4, where the experimental p_s/p values are plotted as a function of the molecular ratio (molar fraction, x) for several salt/solvent combinations. Also plotted for comparison purpose is a curve based on the classic Raoult's law, Eq. (1a). It is clear that, for all types of electrolytes, the p_s/p values follow the Raoult's law prediction until the molar fraction x reaches approximately 0.2, beyond which the vapor pressure rapidly drops to essentially zero (barely detectable). When a vapor pressure is lower than a threshold, no flame would be initiated, and we are proud to state that the present invention provides a platform materials chemistry approach to effectively suppress the initiation of flame.

Although deviations from Raoult's law are not uncommon in science, but this type of curve for the p_s/p values has never been observed for any binary solution systems. In particular, there has been no study reported on the vapor pressure of ultra-high concentration battery electrolytes (with a high molecular fraction, e.g. >0.2 or >0.3) for safety considerations. This is truly unexpected and of technological and scientific significance.

Another surprising element of the present invention is the notion that we are able to dissolve a high concentration of a lithium salt in just about every type of commonly used battery-grade organic solvent to form a quasi-solid electro-

lyte suitable for use in a rechargeable lithium battery. Expressed in a more easily recognizable term, this concentration is typically greater than 3.5 M (mole/liter), more typically and preferably greater than 4 M, still more typically and preferably greater than 5 M, further more preferably greater than 7 M, and most preferably greater than 10 M. Such a high concentration of lithium salt in a solvent has not been generally considered possible. However, one must understand that the vapor pressure of a solution cannot be predicted directly and straightforwardly from the concentration value in terms of M (mole/liter). Instead, for a lithium salt, the molecular ratio x in Raoult's law is the sum of the molar fractions of positive ions and negative ions, which is proportional to the degree of dissociation of a lithium salt in a particular solvent at a given temperature. The mole/liter concentrations do not provide adequate information to enable prediction of vapor pressures.

In general, it has not been possible to achieve such a high concentration of lithium salt (e.g., $x=0.3$-0.7) in an organic solvent used in a battery electrolyte. After an extensive and in-depth study, we came to further discover that the apparent solubility of a lithium salt in a particular solvent could be significantly increased if (a) a highly volatile co-solvent is used to increase the amount of lithium salt dissolved in the solvent mixture first and then (b) this volatile co-solvent is partially or totally removed once the dissolution procedure is completed. Quite unexpectedly, the removal of this co-solvent typically did not lead to precipitation or crystallization of the lithium salt out of the solution even though the solution would have been in a highly supersaturated state. This novel and unique approach appears to have produced a material state wherein most of the solvent molecules are captured or held in place by lithium salt ions that are not volatile (actually the lithium salt being like a solid). Therefore, very few volatile solvent molecules are able to escape into the vapor phase and, hence, very few "flammable" gas molecules are present to help initiate or sustain a flame. This has not been suggested as technically possible or viable in the prior art.

Furthermore, a skilled artisan in the field of chemistry or materials science would have anticipated that such a high salt concentration should make the electrolyte behave like a solid with an extremely high viscosity and, hence, this electrolyte should not be amenable to fast diffusion of lithium ions therein. Consequently, the artisan would have expected that a lithium battery containing such a solid-like electrolyte would not and could not exhibit a high capacity at a high charge-discharge rate or under a high current density condition (i.e. the battery should have a poor rate capability). Contrary to these expectations by a person of ordinary skills or even exceptional skills in the art, all the lithium cells containing such a quasi-solid electrolyte deliver high energy density and high power density for a long cycle life. It appears that the quasi-solid electrolytes as herein invented and disclosed are conducive to facile lithium ion transport. This surprising observation is related to a high lithium ion transference number (TN), to be further explained in a later section of this specification. We have found that the quasi-solid electrolytes provides a TN greater than 0.4 (typically in the range of 0.4-0.8), in contrast to the typical values of 0.1-0.2 in all lower concentration electrolytes (e.g. <2.0 M) used in all current Li-ion and Li—S cells.

As indicated in FIG. 5-8, the Li^+ ion transference number in low salt concentration electrolytes decreases with increasing concentration from $x=0$ to $x=0.2$-0.35. However, beyond molecular ratios of $x=0.2$-0.35, the transference number increases with increasing salt concentration, indicating a

fundamental change in the Li$^+$ ion transport mechanism. Not wishing to be bound by theory, but we would like to offer the following scientifically plausible explanations: When Li$^+$ ions travel in a low salt concentration electrolyte (e.g. x<0.2), each Li$^+$ ion drags one or more solvating anions along with it. The coordinated migration of such a cluster of charged species can be further impeded if the fluid viscosity is increased (i.e. if more salt is added to the solvent).

Fortunately, when an ultra-high concentration of lithium salt (e.g., with x>0.2) is present, Li$^+$ ions could significantly out-number the available solvating anions or solvent molecules that otherwise could cluster the lithium ions, forming multi-ion complex species and slowing down the diffusion process of Li$^+$x ions. This high Li$^+$ ion concentration makes it possible to have more "free Li$^+$ ions" (those acting alone without being clustered), thereby providing a high Li$^+$ transference number (hence, a facile Li$^+$ transport). In other words, the lithium ion transport mechanism changes from a multi-ion complex-dominating one (with a larger hydrodynamic radius) to single ion-dominating one (with a smaller hydrodynamic radius) having a large number of available free Li$^+$ ions. This observation has further asserted that Li$^+$ ions can operate on quasi-solid electrolytes without compromising the rate capability of a lithium-selenium cell. Yet, these highly concentrated electrolytes are non-flammable and safe. These combined features and advantages for battery applications have never been taught or even slightly hinted in any previous report. Theoretical aspects of ion transference number of quasi-solid electrolytes are now presented below:

In selecting an electrolyte system for a battery, the ionic conductivity of lithium ions is an important factor to consider. The ionic conductivity of Li$^+$ ions in an organic liquid-based electrolyte is on the order of 10^{-3}-10^{-2} S/cm and that in a solid state electrolyte is typically in the range of 10^{-4}-10^{-6} S/cm. Due to the low ionic conductivity, solid-state electrolytes have not been used to any significant extent in any battery system. This is a pity since solid-state electrolyte is resistant to dendrite penetration in a lithium metal secondary cell and does not allow for dissolution of lithium polyselenide in a lithium-selenium cell. The charge-discharge capacities of lithium-selenium cells with a solid electrolyte are extremely low. In contrast, the ionic conductivity of our quasi-solid electrolytes is typically in the range of 10^{-4}-8×10^{-3} S/cm, sufficient for use in a rechargeable battery.

The overall ionic conductivity is dictated by the number of charge carriers and the charge carrier mobility of a battery electrolyte. The number of charge carriers, in the lithium battery, is surprisingly dictated by individual transference numbers of cations and anions in the electrolyte. The charge carrier mobility is governed by the viscosity of the electrolyte. For instance, when viscous liquids (hence, lower mobility) are used as electrolytes in lithium batteries, high transference numbers of Li$^+$ ions in the electrolyte are needed.

The ion transport and diffusion in a liquid electrolyte consisting of only one type of cation (i.e. Li$^+$) and one type of anion, plus a liquid solvent or a mixture of two liquid solvents, may be studied by means of AC impedance spectroscopy and pulsed field gradient NMR techniques. The AC impedance provides information about the overall ionic conductivity, and NMR allows for the determination of the individual self-diffusion coefficients of cations and anions. Generally, the self-diffusion coefficients of the cations are slightly higher than those of the anions. The Haven ratio calculated from the diffusion coefficients and the overall

ionic conductivity is typically in the range from 1.3 to 2, indicating that transport of ion pairs or ion complexes (e.g. clusters of Li$^+$-solvating molecules) is an important feature in electrolytes containing a low salt concentration.

The situation becomes more complicated when either two different lithium salts or one ionic liquid (as a lithium salt or liquid solvent) is added to the electrolyte, resulting in a solution having at least 3 or 4 types of ions. In this case, as an example, it is advantageous to use a lithium salt containing the same anion as in the solvating ionic liquid, since the amount of dissolvable lithium salt is higher than in a mixture with dissimilar anions. Thus, the next logical question to ask is whether it is possible to improve the Li$^+$ transference number by dissolving more lithium salt in liquid solvent.

The relation between the overall ionic conductivity of a three-ion liquid mixture, σ_{dc}, and the individual diffusion coefficients of the ions, D_A or D_B, may be given by the Nernst-Einstein equation:

$$\sigma_{dc}=(e^2/k_B T H_R)[(N_{Li}^+)(D_{Li}^+)+(N_A^+)(D_A^+)+(N_B^-)(D_B^-)] \qquad \text{Eq. (2)}$$

Here, e and k_B denote the elementary charge and Boltzmann's constant, respectively, while N_A and N_B are the number densities of individual ions. The Haven ratio, H_R, accounts for cross correlations between the movements of different types of ions.

Simple ionic liquids with only one type of cation and anion are characterized by Haven ratios being typically in the range from 1.3 to 2.0. A Haven ratio larger than unity indicates that ions of dissimilar charges move preferentially into the same direction (i.e. ions transport in pairs or clusters). Evidence for such ion pairs can be found using Raman spectra of various electrolytes. The values for the Haven ratios in the three-ion mixtures are in the range from 1.6 to 2.0. The slightly higher H_R values as compared to the electrolytes with x=0 indicate that pair formation is more prominent in the mixtures.

For the same mixtures, the overall ionic conductivity of the mixtures decreases with increasing lithium salt content x. This conductivity drop is directly related to a drop of the individual self-diffusion coefficients of all ions. Furthermore, studies on different mixtures of ionic liquids with lithium salts have shown that the viscosity increases with increasing lithium salt content x. These findings suggest that the addition of lithium salt leads to stronger ionic bonds in the liquid mixture, which slow down the liquid dynamics. This is possibly due to the Coulomb interaction between the small lithium ions and the anions being stronger than the Coulomb interactions between the larger organic cations and the anions. Thus, the decrease of the ionic conductivity with increasing lithium salt content x is not due to a decreasing number density of mobile ions, but to a decreasing mobility of the ions.

In order to analyze the individual contributions of the cations and anions to the overall ionic conductivity of the mixtures, one may define the apparent transference numbers t_i by:

$$t_i=N_i D i/(\Sigma N_i D i) \qquad \text{Eq. (3)}$$

As an example, in a mixture of N-butyl-N-methyl-pyrrolidinium bis(trifluoromethanesulfonyl) imide (BMP-TFSI) and lithium bis(trifluoromethanesulfonyl)imide (Li-TFSI), containing Li$^+$, BMP$^+$, and TFSI$^-$ ions, the apparent lithium transference number t_{Li} increases with increasing Li-TFSI content; at x=0.377, t_{Li}=0.132 (vs. t_{Li}<0.1 at x<0.2), $D_{Li}\approx0.8D_{TFSI}$, and $D_{BMP}\approx1.6D_{TFSI}$. The main reason for the higher apparent lithium transference number in the mixture is the higher number density of lithium ions.

In order to further enhance the lithium transference number in such mixtures, the number density and/or the diffusion coefficient of the lithium ions have to be further increased relative to the other ions. A further increase of the Li$^+$ ion number density is generally believed to be very challenging since the mixtures tend to undergo salt crystallization or precipitation at high Li salt contents. The present invention has overcome this challenge. We have surprisingly observed that the addition of a very small proportion of a highly volatile organic liquid (e.g. an ether-based solvent) can significantly increase the solubility limit of some Li salt in a highly viscous organic liquid (e.g. VC) or an ionic liquid (e.g. typically from x<0.2 to x>0.3-0.6, or from typically 1-2 M to >5 M). This can be achieved with an ionic liquid (or viscous organic liquid)-to-volatile organic solvent ratio as high as 10:1, hence, keeping the volatile solvent content to a bare minimum and minimizing the potential flammability of the electrolyte.
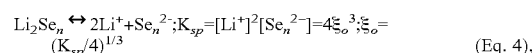
The diffusion coefficients of the ions, as measured in the pulsed field gradient NMR (PFG-NMR) experiments, depend on the effective radius of the diffusing entities. Due to the strong interactions between Li$^+$ ions and TFSI$^+$ ions, Li$^+$ ions can form [Li(TFSI)$_{n+1}$+]$^{n-}$ complexes. Coordination numbers up to n+1=4 have been reported in open literature. The coordination number determines the effective hydrodynamic radius of the complex and thus the diffusion coefficient in the liquid mixture. The Stokes-Einstein equation, Di=k$_B$T/(cπηr$_i$), may be used to calculate the effective hydrodynamic radius of a diffusing entity, ri, from its diffusion coefficient Di. The constant c varies between 4 and 6, depending on the shape of the diffusing entity. A comparison of the effective hydrodynamic radii of cations and anions in ionic liquids with their van der Waals radii reveals that the c values for cations are generally lower than for anions. In the case of EMI-TFSI/Li-TFSI mixtures, hydrodynamic radii for Li are in the range of 0.7-0.9 nm. This is approximately the van der Waals radius of [Li(TFSI)$_2$]$^-$ and [Li(TFSI)$_3$]$^{2-}$ complexes. In the case of the BMP-TFSI/Li-TFSI mixture with x=0.377, the effective hydrodynamic radius of the diffusing lithium complex is r$_{Li}$=(D$_{BMP}$/D$_{Li}$) r$_{BMP}$≈1.1 nm, under the assumption that r$_{BMP}$≈0.55 nm and that the c values for BMP$^+$ and for the diffusing Li complex are identical. This value for r$_{Li}$ suggests that the lithium coordination number in the diffusing complex is at least 2 in the mixtures containing a low salt concentration.

Since the number of TFSI$^-$ ions is not high enough to form a significant amount of [Li(TFSI)$_3$]$^{2-}$ complexes, most lithium ions should be diffusing as [Li(TFSI)$_2$]$^-$ complexes. If, on the other hand, higher Li salt concentrations are achieved without crystallization (e.g. in our quasi-solid electrolytes), then the mixtures should contain a considerable amount of neutral [Li(TFSI)] complexes, which are smaller (r$_{[Li(TFSI)]}$≈0.4 nm) and should have higher diffusivities. Thus, a higher salt concentration would not only enhance the number density of lithium ions but should also lead to higher diffusion coefficients of the diffusing lithium complexes relative to the organic cations. The above analysis is applicable to electrolytes containing either organic liquid solvents or ionic liquid solvents. In all cases, when the lithium salt concentrations are higher than a threshold, there will be an increasing number of free or un-clustered Li$^+$ ions to move between the anode and the cathode when the concentration is further increased, providing adequate amount of Li$^+$ ions required for intercalation/deintercalation or chemical reactions at the cathode and the anode.

In addition to the non-flammability and high lithium ion transference numbers as discussed above, there are several

additional benefits associated with using the presently invented quasi-solid electrolytes. As one example, the quasi-solid electrolyte can significantly enhance cyclic and safety performance of rechargeable lithium batteries through effective suppression of lithium dendrite growth. It is generally accepted that dendrites start to grow in the non-aqueous liquid electrolyte when the anion is depleted in the vicinity of the electrode where plating occurs. In the ultrahigh concentration electrolyte, there is a mass of anions to keep the balance of cations (Li$^+$) and anions near metallic lithium anode. Further, the space charge created by anion depletion is minimal, which is not conducive to dendrite growth. Furthermore, due to both ultrahigh lithium salt concentration and high lithium-ion transference number, the quasi-solid electrolyte provides a large amount of available lithium-ion flux and raises the lithium ionic mass transfer rate between the electrolyte and the lithium electrode, thereby enhancing the lithium deposition uniformity and dissolution during charge/discharge processes. Additionally, the local high viscosity induced by a high concentration will increase the pressure from the electrolyte to inhibit dendrite growth, potentially resulting in a more uniform deposition on the surface of the anode. The high viscosity could also limit anion convection near the deposition area, promoting more uniform deposition of Li ions. These reasons, separately or in combination, are believed to be responsible for the notion that no dendrite-like feature has been observed with any of the large number of rechargeable lithium cells that we have investigated thus far.

As another benefit example, this electrolyte is capable of inhibiting lithium polyselenide and/or polysulfide dissolution at the cathode of a Li—Se or Li—Se/S cell, thus overcoming the polyselenide and/or polysulfide shuttle phenomenon and allowing the cell capacity not to decay significantly with time. Consequently, a coulombic efficiency nearing 100% along with long cycle life has been achieved. The solubility of lithium polyselenide (ξ) is affected by the concentration of lithium ions already present in the electrolyte by the common ion effect. The solubility product (K$_{sp}$) of lithium polyselenide may be written as:

$$\text{Li}_2\text{Se}_n \leftrightarrow 2\text{Li}^+ + \text{Se}_n^{2-}; \text{K}_{sp} = [\text{Li}^+]^2[\text{Se}_n^{2-}] = 4\xi_o^3; \xi_o = (\text{K}_{sp}/4)^{1/3} \tag{Eq. 4},$$

where ξ$_o$ represents the solubility of lithium polyselenide when no lithium ion is present in the solvent. If the concentration of the lithium salt in the electrolyte (C) is significantly larger than the solubility of polyselenide, the solubility of polyselenide in the electrolyte containing the concentrated lithium salt can be expressed as:

$$\xi/\xi_o = (2\xi_o/C)^2 \tag{Eq. 5}.$$

Therefore, when a concentrated electrolyte is used, the solubility of lithium polyselenide will be reduced significantly. This is likely a primary reason why the presently invented quasi-solid electrolyte leads to a lithium-selenium cell with a long and stable cycle life.

The first organic liquid solvent may be selected from the group consisting of 1,3-dioxolane (DOL), 1,2-dimethoxyethane (DME), tetraethylene glycol dimethylether (TEGDME), poly(ethylene glycol) dimethyl ether (PEGDME), diethylene glycol dibutyl ether (DEGDBE), 2-ethoxyethyl ether (EEE), sulfone, sulfolane, ethylene carbonate (EC), dimethyl carbonate (DMC), methylethyl carbonate (MEC), diethyl carbonate (DEC), ethyl propionate, methyl propionate, propylene carbonate (PC), gamma-butyrolactone (γ-BL), acetonitrile (AN), ethyl acetate (EA), propyl formate (PF), methyl formate (MF), toluene, xylene,

methyl acetate (MA), fluoroethylene carbonate (FEC), vinylene carbonate (VC), allyl ethyl carbonate (AEC), a hydrofluoroether (e.g. methyl perfluorobutyl ether, MFE, or ethyl perfluorobutyl ether, EFE), and combinations thereof.

The lithium salt may be selected from lithium perchlorate (LiClO$_4$), lithium hexafluorophosphate (LiPF$_6$), lithium borofluoride (LiBF$_4$), lithium hexafluoroarsenide (LiAsF$_6$), lithium trifluoro-metasulfonate (LiCF$_3$SO$_3$), bis-trifluorom-ethyl sulfonylimide lithium (LiN(CF$_3$SO$_2$)$_2$), lithium bis (oxalato)borate (LiBOB), lithium oxalyldifluoroborate (LiBF$_2$C$_2$O$_4$), lithium oxalyldifluoroborate (LiBF$_2$C$_2$O$_4$), lithium nitrate (LiNO$_3$), Li-Fluoroalkyl-Phosphates (LiPF$_3$ (CF$_2$CF$_3$)$_3$), lithium bisperfluoro-ethysulfonylimide (Li-BETI), lithium bis(trifluoromethanesulphonyl)imide, lithium bis(fluorosulphonyl)imide, lithium trifluorometh-anesulfonimide (LiTFSI), an ionic liquid lithium salt, or a combination thereof.

The ionic liquid is composed of ions only. Ionic liquids are low melting temperature salts that are in a molten or liquid state when above a desired temperature. For instance, an ionic salt is considered as an ionic liquid if its melting point is below 100° C. If the melting temperature is equal to or lower than room temperature (25° C.), the salt is referred to as a room temperature ionic liquid (RTIL). The IL-based lithium salts are characterized by weak interactions, due to the combination of a large cation and a charge-delocalized anion. This results in a low tendency to crystallize due to flexibility (anion) and asymmetry (cation).

Some ILs may be used as a co-solvent (not as a salt) to work with the first organic solvent of the present invention. A well-known ionic liquid is formed by the combination of a 1-ethyl-3-methyl-imidazolium (EMI) cation and an N,N-bis(trifluoromethane)sulphonamide (TFSI) anion. This com-bination gives a fluid with an ionic conductivity comparable to many organic electrolyte solutions, a low decomposition propensity and low vapor pressure up to ~300-400° C. This implies a generally low volatility and non-flammability and, hence, a much safer electrolyte solvent for batteries.

Ionic liquids are basically composed of organic or inor-ganic ions that come in an unlimited number of structural variations owing to the preparation ease of a large variety of their components. Thus, various kinds of salts can be used to design the ionic liquid that has the desired properties for a given application. These include, among others, imidazo-lium, pyrrolidinium and quaternary ammonium salts as cations and bis(trifluoromethanesulphonyl) imide, bis(fluo-rosulphonyl)imide and hexafluorophosphate as anions. Use-ful ionic liquid-based lithium salts (not solvent) may be composed of lithium ions as the cation and bis(trifluo-romethanesulphonyl)imide, bis(fluorosulphonyl)imide and hexafluorophosphate as anions. For instance, lithium trif-luoromethanesulfonimide (LiTFSI) is a particularly useful lithium salt.

Based on their compositions, ionic liquids come in dif-ferent classes that include three basic types: aprotic, protic and zwitterionic types, each one suitable for a specific application. Common cations of room temperature ionic liquids (RTILs) include, but are not limited to, tetraalky-lammonium, di, tri, and tetra-alkylimidazolium, alkylpyri-dinium, dialkyl-pyrrolidinium, dialkylpiperidinium, tet-raalkylphosphonium, and trialkylsulfonium. Common anions of RTILs include, but are not limited to, BF$_4^-$, B(CN)$_4^-$, CH$_3$BF$_3^-$, CH$_2$CHBF$_3^-$, CF$_3$BF$_3^-$, C$_2$F$_5$BF$_3^-$, n-C$_3$F$_7$BF$_3^-$, n-C$_4$F$_9$BF$_3^-$, PF$_6^-$, CF$_3$CO$_2^-$, CF$_3$SO$_3^-$, N(SO$_2$CF$_3$)$_2^-$, N(COCF$_3$)(SO$_2$CF$_3$)$^-$, N(SO$_2$F)$_2^-$, N(CN)$_2^-$, C(CN)$_3^-$, SCN$^-$, SeCN$^-$, CuCl$_2^-$, AlCl$_4^-$, F(HF)$_{2.3}^-$, etc. Relatively speaking, the combination of imidazolium- or

sulfonium-based cations and complex halide anions such as AlCl$_4^-$, BF$_4^-$, CF$_3$CO$_2^-$, CF$_3$SO$_3^-$, NTf$_2^-$, N(SO$_2$F)$_2^-$, or F(HF)$_{2.3}^-$ results in RTILs with good working conductivi-ties.

RTILs can possess archetypical properties such as high intrinsic ionic conductivity, high thermal stability, low vola-tility, low (practically zero) vapor pressure, non-flammabil-ity, the ability to remain liquid at a wide range of tempera-tures above and below room temperature, high polarity, high viscosity, and wide electrochemical windows. These prop-erties, except for the high viscosity, are desirable attributes when it comes to using an RTIL as an electrolyte co-solvent in a rechargeable lithium cell.

The anode active material may contain, as an example, lithium metal foil or a high-capacity Si, Sn, or SnO$_2$ capable of storing a great amount of lithium.

Typically, the cathode active materials are not electrically conducting. Hence, in one embodiment, the cathode active material may be mixed with a conductive filler such as carbon black (CB), acetylene black (AB), graphite particles, expanded graphite particles, activated carbon, meso-porous carbon, meso-carbon micro bead (MCMB), carbon nano-tube (CNT), carbon nano-fiber (CNF), graphene sheet (also referred to as nano graphene platelet, NGP), carbon fiber, or a combination thereof. These carbon/graphite/graphene materials may be made into a form of fabric, mat, or paper for supporting the cathode active material.

In a preferred embodiment, the nano-scaled filaments (e.g. CNTs, CNFs, and/or NGPs) are formed into a porous nano-structure that contains massive surfaces to support either the anode active material (e.g. Li or Si coating) or the cathode active material (e.g. selenium, selenium-sulfur alloy or mixture, etc). The porous nano-structure should have pores having a pore size preferably from 2 nm to 1 μm prior to being impregnated with selenium, Se/S, or selenium polysulfide. The pore size is preferably in the range of 2 nm-50 nm, further preferably 2 nm-0 nm, after the pores are impregnated with Se or lithium polyselenide. These pores are properly sized to accommodate the electrolyte at the cathode side and to retain the cathode active material in the pores during repeated charges/discharges. The same type of nano-structure may be implemented at the anode side to support the anode active material.

In another preferred embodiment, the cathode active material consists of (a) exfoliated graphite worms that are interconnected to form a porous, conductive graphite flake network comprising pores having a size smaller than 100 nm; and (b) nano-scaled powder or coating of Se, Se/S alloy or mixture, or lithium polyselenide/polysulfide disposed in the pores or coated on a graphite flake surface wherein the powder or coating is in contact with the electrolyte and has a dimension less than 100 nm. Preferably, the exfoliated graphite worm amount is in the range of 1% to 90% by weight and the amount of powder or coating is in the range of 99% to 10% by weight based on the total weight of exfoliated graphite worms and Se, Se/S, or lithium poly-selenide/polysulfide combined which is measured or calcu-lated when the cell is in a fully charged state. Preferably, the amount of the powder or coating of Se, Se/S, or lithium polyselenide/polysulfide is in the range of 70% to 95% by weight. Most preferably, the amount of the powder or coating of Se, Se/S, or lithium polyselenide/polysulfide is no less than 80% by weight.

The electrons coming from or going out through the external load or circuit must go through the conductive additives (in a conventional sulfur cathode) or a conductive framework (e.g. exfoliated graphite meso-porous structure

or nano-structure of conductive nano-filaments) to reach the cathode active material. Since the cathode active material (e.g. Se, Se/S, or lithium polyselenide/polysulfide) is a poor electronic conductor, the active material particle or coating must be as thin as possible to reduce the required electron travel distance.

We have recently found that the cathode active material utilization rate is a serious problem in the Li—S cell. We now found that this is a big problem for Li—Se cells as well even though Se, as a semiconductor, has an electrical conductivity (10^{-5} S/cm) higher than that (5×10^{-30} S/cm) of Li—S cells by 24 orders of magnitude. In conventional Li—S cells, the cathode active material (S) is typically limited to less than 70% by weight of the composite cathode, which is composed of sulfur and the conductive additive/support. Even when the sulfur content in the prior art composite cathode reaches or exceeds 70% by weight, the specific capacity of the composite cathode is typically significantly lower than what can be expected based on theoretical predictions. For instance, the theoretical specific capacity of sulfur is 1,675 mAh/g. Thus, a composite cathode composed of 70% sulfur (S) and 30% carbon black (CB), without any binder, should be capable of storing up to $1,675 \times 70\% = 1,172$ mAh/g. Unfortunately, the actually observed specific capacity is typically less than 75% (often less than 50%) of what can be achieved. In other words, the active material utilization rate is typically less than 75% (or even <50%). This has been a major issue in the art of Li—S cells and we have also found that Li—Se and Li—Se/S cells have a similar issue, and there has been no solution to this problem. Most surprisingly, the implementation of exfoliated graphite worms as a conductive supporting material for sulfur, selenium, or Se/S alloy, coupled with a quasi-solid electrolyte at the cathode, has made it possible to achieve an active material utilization rate of typically >>80%, more often greater than 90%, and, in many cases, close to 99%.

In the presently invented lithium-selenium cell, the pores of the porous sulfur/exfoliated graphite mixture or composite preferably have a size from 2 nm to 10 nm to accommodate electrolyte therein after the nano-scaled powder or coating of Se, Se/S, lithium polyselenide, and/or lithium polysulfide is disposed in the pores or coated on the graphite flake surface. These pore sizes in the sulfur/exfoliated graphite mixture or composite are surprisingly capable of further suppressing, reducing, or eliminating the shuttle effect. Not wishing to be bound by the theory, but we feel that this is likely due to the unexpected capability of exfoliated graphite flake surfaces spaced 2-10 nm apart to retain lithium polysulfides in the minute pockets (pores) during the charge and discharge cycles. This ability of graphitic surfaces to prevent out-migration of lithium polysulfide is another big surprise to us.

The exfoliated graphite worms can be obtained from the intercalation and exfoliation of a laminar graphite material. The conventional process for producing exfoliated graphite worms typically begins with subjecting a graphitic material to a chemical treatment (intercalation and/or oxidation using a strong acid and/or oxidizing agent) to form a graphite intercalation compound (GIC) or graphite oxide (GO). This is most often accomplished by immersing natural graphite powder in a mixture of sulfuric acid, nitric acid (an oxidizing agent), and another oxidizing agent (e.g. potassium permanganate or sodium chlorate). The resulting GIC is actually some type of graphite oxide (GO) particles. This GIC is then repeatedly washed and rinsed in water to remove excess acids, resulting in a graphite oxide suspension or dispersion, which contains discrete and visually discernible graphite

oxide particles dispersed in water. There are different processing routes that can be followed after this rinsing step to form different types of graphite or graphene products.

For instance, a first route involves removing water from the suspension to obtain "expandable graphite," which is essentially a mass of dried GIC or dried graphite oxide particles. Upon exposure of expandable graphite to a temperature in the range of typically 800-1,050° C. for approximately 30 seconds to 2 minutes, the GIC undergoes a rapid expansion by a factor of 30-800 to form "graphite worms", which are each a collection of exfoliated, but largely unseparated or still interconnected graphite flakes.

As a second route, one may choose to use a low-intensity air mill or shearing machine to simply break up the graphite worms for the purpose of producing the so-called "expanded graphite flakes," which are isolated and separated graphite flakes or platelets thicker than 100 nm (hence, not a nano material by definition). Alternatively, exfoliated graphite worms may be the re-compressed (e.g. roll-pressed) to form flexible graphite sheet or flexible graphite foil that is essentially a solid film not permeable to battery electrolyte. Such an electrolyte-impermeable film can be a good battery current collector (e.g. to replace aluminum foil), but it does not have a sufficient amount of specific surface area to support sulfur.

Alternatively, as a third route, the exfoliated graphite worms may be subjected to high-intensity mechanical shearing (e.g. using an ultrasonicator, high-shear mixer, high-intensity air jet mill, or high-energy ball mill) to form separated single-layer and/or multi-layer graphene sheets (collectively called nano graphene platelets or NGPs), as disclosed in our U.S. application Ser. No. 10/858,814. Single-layer graphene can be as thin as 0.34 nm, while multi-layer graphene can have a thickness up to 100 nm.

The graphite oxide suspension (after a sufficiently high degree of oxidation) may be subjected to ultrasonication for the purpose of separating/isolating individual graphene oxide sheets from graphite oxide particles. This is based on the notion that the inter-graphene plane separation bas been increased from 0.335 nm in natural graphite to 0.6-1.1 nm in highly oxidized graphite oxide, significantly weakening the van der Waals forces that hold neighboring planes together. Ultrasonic power can be sufficient to further separate graphene plane sheets to form separated, isolated, or discrete graphene oxide (GO) sheets having an oxygen content of typically 20-50% by weight. These graphene oxide sheets can then be chemically or thermally reduced to obtain "reduced graphene oxides" (RGO) typically having an oxygen content of 0.01%-10% by weight, more typically 0.01%-5% by weight, and most typically 0.01%-2% by weight.

In general, NGPs include single-layer and multi-layer graphene or reduced graphene oxide with an oxygen content of 0-10% by weight, more typically 0-5% by weight, and preferably 0-2% weight. Pristine graphene has essentially 0% oxygen. Graphene oxide (including RGO) can have 0.01%-50% by weight of oxygen.

As indicated earlier, dried GIC or GO powder may be exposed a thermal shock (at a high temperature, typically 800-1,050° C.) for a short period of time (typically 30-120 seconds), allowing the constituent graphite flakes to freely expand. The resulting graphite worms typically have an expanded volume that is 30 to 800 times higher than the original graphite volume, depending upon the degree of oxidation or intercalation.

Typically, an oxygen content between 46-50% by weight based on the total GO weight is an indication of practically

complete oxidation of graphite, which is also reflected by the complete disappearance of the X-ray diffraction curve peak originally located at 2θ=approximately 26 degrees for un-intercalated or un-oxidized natural graphite. This diffraction peak at 2θ=approximately 26 degrees corresponds to the d_{002} spacing between two (002) graphene planes.

Acids, such as sulfuric acid, are not the only type of intercalating agent (intercalant) that penetrate into spaces between graphene planes. Many other types of intercalating agents, such as alkali metals (Li, K, Na, Cs, and their alloys or eutectics), can be used to intercalate graphite to stage 1, stage 2, stage 3, etc. Stage n implies one intercalant layer for every n graphene planes. For instance, a stage-1 potassium-intercalated GIC means there is one layer of K for every graphene plane; or, one can find one layer of K atoms inserted between two adjacent graphene planes in a G/K/G/K/G/KG . . . sequence, where G is a graphene plane and K is a potassium atom plane. A stage-2 GIC will have a sequence of GG/K/GG/K/GG/K/GG . . . and a stage-3 GIC will have a sequence of GGG/K/GGG/K/GGG . . . , etc.

A graphite worm is characterized as having a network of largely interconnected exfoliated graphite flaks with pores between flakes. The flakes have a typical length or width dimension of 0.5-100 µm (more typically 1-20 µm), depending upon the types of starting graphitic materials used and these lateral dimensions (length or width) are relatively independent of the GIC stage number (or oxygen content in GO), the exfoliation temperature, and the exfoliation environment. However, these factors have major impact on the volume expansion ratio (exfoliated graphite worm volume vs. starting graphite particle volume), flake thickness range, and pore size range of exfoliated graphite worms.

For instance, Stage-1 GIC or fully oxidized graphite (GO with 40-50% oxygen content), upon un-constrained exfoliation at 1,000° C. for one minute, exhibit a typical volume expansion ratio of approximately 450-800%, flake thickness range of 0.34 to 3 nm, and pore size range of 50 nm to 20 µm. By contrast, Stage-5 GIC or GO with 20-25% oxygen content, upon un-constrained exfoliation at 1,000° C. for one minute, exhibit a volume expansion ratio of approximately 80-180%, flake thickness range of 1.7 to 200 nm, and pore size range of 30 nm to 2 µm.

Stage-1 GIC is the most desirable since it leads to highly exfoliated graphite worms featuring thin graphite flakes with very high specific surface areas (typically >500 m²/g, often >700 m²/g, and even >1,000 m²/g in several cases). Higher surface areas make it possible to deposit thinner sulfur or lithium polysulfide coating given the same sulfur or lithium polysulfide volume. Consequently, there is significantly reduced proportion of thicker coating of sulfur or lithium polysulfide attached to the exfoliated graphite flake surfaces. This could allow most of the sulfur to be accessible to the lithium ions during the cell discharge.

The flakes in an exfoliated graphite worm remain substantially interconnected (physically in contact with each other or bonded to each other), forming a network of electron-conducting paths. Hence, the electrical conductivity of the graphite worms is relatively high (10-10,000 S/cm), which can be orders of magnitude higher than that of carbon black, activated carbon, polymeric carbon, amorphous carbon, hard carbon, soft carbon, and meso-phase pitch, etc.

The soft and fluffy worms, upon impregnation or coating with sulfur, have exhibited an unexpected improvement in mechanical strength (e.g. compression strength or bending strength) by up to 2-3 orders of magnitude. The impregnated graphite worms may be re-compressed to increase their

physical density and structural integrity, if deemed necessary. Graphite worm-sulfur composites have a density typically in the range of 0.02 g/cm³ to 1.0 g/cm³, depending upon the degree of exfoliation and the condition of re-compression.

When the cathode is made, the cathode active material (sulfur, lithium polysulfide, vanadium oxide, titanium disulfide, etc) is embedded in the nano-scaled pores constituted by the exfoliated graphite flakes. Preferably, the cathode active material is grinded into nanometer scale (preferably <10 nm and more preferably <5 nm). Alternatively, the cathode active material may be in a thin-film coating form deposited on surfaces of the graphite flakes obtained by melt impregnation, solution deposition, electro-deposition, chemical vapor deposition (CVD), physical vapor deposition, sputtering, laser ablation, etc. This coating is then brought in contact with electrolyte before, during, or after the cathode is made, or even after the cell is produced.

The present design of a meso-porous graphite worm cathode with meso-scaled pores in a Li—S cell was mainly motivated by the notion that a significant drawback with cells containing cathodes comprising elemental sulfur, organosulfur and carbon-sulfur materials is related to the dissolution and excessive out-diffusion of soluble sulfides, polysulfides, organo-sulfides, carbon-sulfides and/or carbon-polysulfides (anionic reduction products) from the cathode into the rest (anode, in particular) of the cell. This process leads to several problems: high self-discharge rates, loss of cathode capacity, corrosion of current collectors and electrical leads leading to loss of electrical contact to active cell components, fouling of the anode surface giving rise to malfunction of the anode, and clogging of the pores in the cell membrane separator which leads to loss of ion transport and large increases in internal resistance in the cell.

At the anode side, when lithium metal is used as the sole anode active material in a Li metal cell, there is concern about the formation of lithium dendrites, which could lead to internal shorting and thermal runaway. Herein, we have used two approaches, separately or in combination, to addressing this dendrite formation issue: one involving the use of a high-concentration electrolyte and the other the use of a nano-structure composed of conductive nano-filaments. For the latter, multiple conductive nano-filaments are processed to form an integrated aggregate structure, preferably in the form of a closely packed web, mat, or paper, characterized in that these filaments are intersected, overlapped, or somehow bonded (e.g., using a binder material) to one another to form a network of electron-conducting paths. The integrated structure has substantially interconnected pores to accommodate electrolyte. The nano-filament may be selected from, as examples, a carbon nano fiber (CNF), graphite nano fiber (GNF), carbon nano-tube (CNT), metal nano wire (MNW), conductive nano-fibers obtained by electro-spinning, conductive electro-spun composite nano-fibers, nano-scaled graphene platelet (NGP), or a combination thereof. The nano-filaments may be bonded by a binder material selected from a polymer, coal tar pitch, petroleum pitch, meso-phase pitch, coke, or a derivative thereof.

Surprisingly and significantly, the nano-structure provides an environment that is conducive to uniform deposition of lithium atoms, to the extent that no geometrically sharp structures or dendrites were found in the anode after a large number of cycles. Not wishing to be bound by any theory, but the applicants envision that the 3-D network of highly conductive nano-filaments provide a substantially uniform attraction of lithium ions back onto the filament surfaces during re-charging. Furthermore, due to the nanometer sizes

of the filaments, there is a large amount of surface area per unit volume or per unit weight of the nano-filaments. This ultra-high specific surface area offers the lithium ions an opportunity to uniformly deposit a lithium metal coating on filament surfaces at a high rate, enabling high re-charge rates for a lithium metal secondary battery.

The presently invented high-concentration electrolyte system and optional meso-porous exfoliated graphite-sulfur may be incorporated in rechargeable lithium-selenium cells:

(A) Lithium metal-selenium (Li—Se and Li—Se/S) with a conventional anode configuration: The cell contains an optional cathode current collector, a cathode (containing a composite of Se, Se/S, or lithium polyselenide/polysulfide and a conductive additive or a conductive supporting framework, such as a meso-porous exfoliated graphite or a nano-structure of conductive nano-filaments), a separator/electrolyte (featuring the gradient electrolyte system), and an anode current collector. Potential dendrite formation may be overcome by using the high-concentration electrolyte (quasi-solid electrolyte) at the anode.

(B) Lithium metal-selenium (Li—Se and Li—Se/S) cell with a nano-structured anode configuration: The cell contains an optional cathode current collector, a cathode (containing a composite of Se, Se/S, or lithium polyselenide/polysulfide and a conductive additive or a conductive supporting framework, such as a meso-porous exfoliated graphite or a nano-structure of conductive nano-filaments), a separator/electrolyte (featuring the gradient electrolyte system), an optional anode current collector, and a nano-structure to accommodate lithium metal that is deposited back to the anode during a charge or re-charge operation. This nano-structure (web, mat, or paper) of nano-filaments provide a uniform electric field enabling uniform Li metal deposition, reducing the propensity to form dendrites. This configuration, coupled with the high-concentration electrolyte at the anode, provides a dendrite-free cell for a long and safe cycling behavior.

(C) Lithium ion-selenium cell with a conventional anode: For instance, the cell contains an anode composed of anode active graphite particles bonded by a binder, such as polyvinylidene fluoride (PVDF) or styrenebutadiene rubber (SBR). The cell also contains a cathode current collector, a cathode (containing a composite of Se, Se/S, or lithium polyselenide/polysulfide and a conductive additive or a conductive supporting framework, such as a meso-porous exfoliated graphite or a nano-structure of conductive nano-filaments), a separator/electrolyte (featuring the quasi-solid electrolyte system), and an anode current collector, and

(D) Lithium ion-selenium cell with a nano-structured anode: For instance, the cell contains a web of nanofibers coated with Si coating or bonded with Si nano particles. The cell also contains an optional cathode current collector, a cathode (containing a composite of Se, Se/S, or lithium polyselenide/polysulfide and a conductive additive or a conductive supporting framework, such as a meso-porous exfoliated graphite or a nano-structure of conductive nano-filaments), a separator/electrolyte (featuring the quasi-solid electrolyte system), and an anode current collector. This configuration provides an ultra-high capacity, high energy density, and a safe and long cycle life.

In the lithium-ion selenium cell (e.g. as described in (C) and (D) above), the anode active material can be selected from a wide range of high-capacity materials, including (a)

silicon (Si), germanium (Ge), tin (Sn), lead (Pb), antimony (Sb), bismuth (Bi), zinc (Zn), aluminum (Al), nickel (Ni), cobalt (Co), manganese (Mn), titanium (Ti), iron (Fe), and cadmium (Cd), and lithiated versions thereof; (b) alloys or intermetallic compounds of Si, Ge, Sn, Pb, Sb, Bi, Zn, Al, or Cd with other elements, and lithiated versions thereof, wherein said alloys or compounds are stoichiometric or non-stoichiometric; (c) oxides, carbides, nitrides, sulfides, phosphides, selenides, and tellurides of Si, Ge, Sn, Pb, Sb, Bi, Zn, Al, Fe, Ni, Co, Ti, Mn, or Cd, and their mixtures or composites, and lithiated versions thereof; (d) salts and hydroxides of Sn and lithiated versions thereof; (e) carbon or graphite materials and prelithiated versions thereof; and combinations thereof. Non-lithiated versions may be used if the cathode side contains lithium polysulfides or other lithium sources when the cell is made.

A possible lithium-selenium cell may be comprised of an anode current collector, an electrolyte phase (optionally but preferably supported by a porous separator, such as a porous polyethylene-polypropylene co-polymer film), a meso-porous exfoliated graphite worm (EGW)-Se/S or EGW-Se cathode of the instant invention (containing a cathode active material, Se/S or Se), and an optional cathode collector. This cathode current collector is optional because the presently invented meso-porous exfoliated graphite structure, if properly designed, can act as a current collector or as an extension of a current collector.

To achieve high capacity in a battery, it is desirable to have either a higher quantity or loading of the cathode active material or, preferably, a higher-capacity cathode active material in the cathode layer. Lithium and Se or Se/S are highly desirable as the electrochemically active materials for the anode and cathode, respectively, because they provide exceptionally high energy density on a weight or volume basis. To obtain high energy densities, the lithium can be present as the pure metal, in an alloy (in a lithium-metal cell), or in an intercalated form (in a lithium-ion cell), and the Se can be present as elemental selenium or as a component in an organic or inorganic material with a high Se content.

In order to solve the poor electrical conductivity issue of Se and Se/S cathode, presumably one could choose to use carbon paper (instead of or in addition to carbon black) as a host for the cathode active material. However, this conventional carbon fiber paper does not allow for a sufficient amount of cathode active material to be coated on the large-diameter carbon fiber surface yet still maintaining a low coating thickness, which is required of a reduced lithium diffusion path length for improved charge/discharge rates and reduced resistance. In other words, in order to have a reasonable proportion of an electrode active material coated on a large-diameter fiber, the coating thickness has to be proportionally higher. A thicker coating would mean a longer diffusion path for lithium to come in and out, thereby slowing down the battery charge/discharge rates. The instant application solved these challenging problems by using an integrated 3-D meso-porous graphite worm structure consisting of nano-thickness exfoliated graphite flakes having massive conductive surfaces to host the cathode active material.

As opposed to carbon paper that was composed of micron-scaled carbon fibers (typically having a diameter of >12 μm), the instant application makes use of graphite worms of nano-thickness flakes with a thickness less than 200 nm, preferably and more typically less than 100 nm, even more preferably and more typically less than 10 nm, and most preferably and more typically less than 3 nm. The

exfoliated graphite worms have been ignored or overlooked by the workers in the art of designing electrodes likely due to the notion that these worms are perceived as too weak to be handled in an electrode-making process and too weak to support any sulfur-containing electrode active material. Indeed, graphite worms are extremely weak. However, impregnation of coating of graphite worms with Se or Se/S alloy or mixture significantly enhances the mechanical strength of graphite worms, to the extent that the resulting composite materials can be readily formed into a cathode using a conventional battery electrode-making machine (coater). Further, there has been no teaching that exfoliated graphite worms could be used to confine lithium polyselenide/polysulfide and preventing lithium polyselenide/polysulfide from migrating out of the cathode and entering the anode. This was not trivial or obvious to one of ordinary skills in the art.

The interconnected network of exfoliated graphite worms forms a continuous path for electrons, resulting in significantly reduced internal energy loss or internal heating for either the anode or the cathode (or both). This network is electronically connected to a current collector and, hence, all graphite flakes that constitute graphite worms are essentially connected to the current collector. In the instant invention, the lithium sulfide coating is deposited on flake surfaces and, even if the coating were to fracture into separate segments, individual segments would still remain in physical contact with the underlying flakes, which is essentially part of the current collector. The electrons transported to the cathode can be distributed to all cathode active coatings. In the case of lithium selenide/sulfide particles dispersed/dissolved in an electrolyte inside meso pores of the cathode structure, the particles are necessarily nano-scaled (the salt-electrolyte solution pool also nano-scaled) and, hence, are conducive to fast cathode reaction during the charging operation.

The lithium metal cell of the instant application can have a nano-structured anode or a more conventional anode structure, although such a conventional structure is not preferred. In a more conventional anode structure, acetylene black, carbon black, or ultra-fine graphite particles may be used as a conductive additive. The binder may be chosen from polytetrafluoroethylene (PTFE), polyvinylidene fluoride (PVDF), ethylene-propylene-diene copolymer (EPDM), or styrene-butadiene rubber (SBR), for example. Conductive materials such as electronically conductive polymers, meso-phase pitch, coal tar pitch, and petroleum pitch may also be used as a binder. Preferable mixing ratio of these ingredients may be 80 to 95% by weight for the anode active material (natural or artificial graphite particles, MCMBs, coke-based anode particles, carbon-coated Si nano particles, etc), 3 to 20% by weight for the conductive additive, and 2 to 7% by weight for the binder. The anode current collector may be selected from copper foil or stainless steel foil. The cathode current collector may be an aluminum foil or a nickel foil. There is no particularly significant restriction on the type of current collector, provided the material is a good electrical conductor and relatively corrosion resistant. The separator may be selected from a polymeric nonwoven fabric, porous polyethylene film, porous polypropylene film, or porous PTFE film.

The most important property of a filament herein used to support an electrode active material (e.g. Li or Si at the anode) is a high electrical conductivity to enable facile transport of electrons with minimal resistance. A low conductivity implies a high resistance and high energy loss, which is undesirable. The filament should also be chemically and thermo-mechanically compatible with the intended

active material (i.e., lithium at the anode) to ensure a good contact between the filament and the coating upon repeated charging/discharging and heating/cooling cycles. Several techniques can be employed to fabricate a conductive aggregate of filaments (a web or mat), which is a monolithic body having desired interconnected pores. In one preferred embodiment of the present invention, the porous web can be made by using a slurry molding or a filament/binder spraying technique. These methods can be carried out in the following ways:

EXAMPLES

In the examples discussed below, unless otherwise noted, raw materials such as silicon, germanium, bismuth, antimony, zinc, iron, nickel, titanium, cobalt, and tin were obtained from either Alfa Aesar of Ward Hill, Mass., Aldrich Chemical Company of Milwaukee, Wis. or Alcan Metal Powders of Berkeley, Calif. X-ray diffraction patterns were collected using a diffractometer equipped with a copper target x-ray tube and a diffracted beam monochromator. The presence or absence of characteristic patterns of peaks was observed for each of the alloy samples studied. For example, a phase was considered to be amorphous when the X-ray diffraction pattern was absent or lacked sharp, well-defined peaks. In several cases, scanning electron microscopy (SEM) and transmission electron microscopy (TEM) were used to characterize the structure and morphology of the hybrid material samples.

A nano-structured cathode, comprising exfoliated graphite worm-Se (Se/S or lithium polyselenide/polysulfide), was bonded onto an aluminum foil (a current collector). After solvent removal, web-aluminum foil configuration was hot-pressed to obtain a cathode or, alternatively, a complete cell was fabricated by laminating an anode current collector (Cu foil), an anode layer (e.g., a piece of Li foil, a nano-structured web with Si coating, or graphite particles bonded by PVDF), an electrolyte-separator layer, a meso-porous cathode, and a cathode current collector (e.g., stainless steel foil or aluminum foil) all at the same time. In some cases, an NGP-containing resin was used as a binder, for instance, between a cathode layer and a cathode current collector. Filaments may also be bonded by an intrinsically conductive polymer as a binder to form a web. For instance, polyaniline-maleic acid-dodecyl hydrogensulfate salt may be synthesized directly via emulsion polymerization pathway using benzoyl peroxide oxidant, sodium dodecyl sulfate surfactant, and maleic acid as dopants. Dry polyaniline-based powder may be dissolved in DMF up to 2% w/v to form a solution.

The conventional cathode of a Li—Se cell was prepared in the following way. As an example, 60-80% by weight of lithium selenide powder, 3.5% by weight of acetylene black, 13.5-33.5% by weight of graphite, and 3% by weight of ethylene-propylene-diene monomer powder were mixed together with toluene to obtain a mixture. The mixture was then coated on an aluminum foil (30 μm) serving as a current collector. The resulting two-layer aluminum foil-active material configuration was then hot-pressed to obtain a positive electrode. In the preparation of a cylindrical cell, a positive electrode, a separator composed of a porous polyethylene film, and a negative electrode was stacked in this order. The stacked body was spirally wound with a separator layer being disposed at the outermost side to obtain an electrode assembly. Li-ion selenium cells were similarly made wherein, for instance, the cathode is prepared by

mixing 90% by weight of a selected cathode active material with 5% conductive additive (e.g. carbon black), and 5% binder (e.g. PVDF).

The following examples are presented primarily for the purpose of illustrating the best mode practice of the present invention, not to be construed as limiting the scope of the present invention.

Example 1: Some Examples of Electrolytes Used

A wide range of lithium salts can be used as the lithium salt dissolved in an organic liquid solvent (alone or in a mixture with another organic liquid or an ionic liquid). The following are good choices for lithium salts that tend to be dissolved well in selected organic or ionic liquid solvents: lithium borofluoride ($LiBF_4$), lithium trifluoro-metasulfonate ($LiCF_3SO_3$), lithium bis-trifluoromethyl sulfonylimide ($LiN(CF_3SO_2)_2$ or LITFSI), lithium bis(oxalato)borate (LiBOB), lithium oxalyldifluoroborate ($LiBF_2C_2O_4$), and lithium bisperfluoroethy-sulfonylimide (LiBETI). A good electrolyte additive for helping to stabilize Li metal is $LiNO_3$. Particularly useful ionic liquid-based lithium salts include: lithium bis(trifluoro methanesulfonyl)imide (LiTFSI).

Preferred organic liquid solvents include: ethylene carbonate (EC), dimethyl carbonate (DMC), methylethyl carbonate (MEC), diethyl carbonate (DEC), propylene carbonate (PC), acetonitrile (AN), vinylene carbonate (VC), allyl ethyl carbonate (AEC), 1,3-dioxolane (DOL), 1,2-dimethoxyethane (DME), tetraethylene glycol dimethylether (TEGDME), Poly(ethylene glycol) dimethyl ether (PEGDME), diethylene glycol dibutyl ether (DEGDBE), 2-ethoxyethyl ether (EEE), hydrofluoroether (e.g. TPTP), sulfone, and sulfolane.

Preferred ionic liquid solvents may be selected from a room temperature ionic liquid (RTIL) having a cation selected from tetraalkylammonium, di-alkylimidazolium, alkylpyridinium, dialkyl-pyrrolidinium, or dialkylpiperidinium. The counter anion is preferably selected from BF_4^-, $B(CN)_4^-$, $CF_3CO_2^-$, $CF_3SO_3^-$, $N(SO_2CF_3)_2^-$, $N(COCF_3)$ $(SO_2CF_3)^-$, or $N(SO_2F)_2^-$. Particularly useful ionic liquid-based solvents include N-n-butyl-N-ethylpyrrolidinium bis (trifluoromethane sulfonyl)imide (BEPyTFSI), N-methyl-N-propylpiperidinium bis(trifluoromethyl sulfonyl)imide

($PP_{13}TFSI$), and N,N-diethyl-N-methyl-N-(2-methoxy-ethyl) ammonium bis(trifluoromethylsulfonyl)imide.

Example 2: Vapor Pressure of Some Solvents and Corresponding Quasi-Solid Electrolytes with Various Lithium Salt Molecular Ratios

Vapor pressures of several solvents (DOL, DME, PC, AN, with or without an ionic liquid-based co-solvent, $PP_{13}TFSI$) before and after adding a wide molecular ratio range of lithium salts, such as lithium borofluoride ($LiBF_4$), lithium trifluoro-metasulfonate ($LiCF_3SO_3$), or bis(trifluoro methanesulfonyl)imide (LiTFSI), were measured. Some of the vapor pressure ratio data (p/p=vapor pressure of solution/ vapor pressure of solvent alone) are plotted as a function of the lithium salt molecular ratio x, as shown in FIG. 1-4, along with a curve representing the Raoult's Law. In all cases, the vapor pressure ratio follows the theoretical prediction based on Raoult's Law for up to x<0.15 only, above which the vapor pressure deviates from Raoult's Law in a novel and unprecedented manner. It appears that the vapor pressure drops at a very high rate when the molecular ratio x exceeds 0.2, and rapidly approaches a minimal or essentially zero when x exceeds 0.4. With a very low p_s/p value, the vapor phase of the electrolyte either cannot ignite or cannot sustain a flame for longer than 3 seconds once initiated.

Example 3: Flash Points and Vapor Pressure of Some Solvents and Corresponding Quasi-Solid Electrolytes with a Lithium Salt Molecular Ratio of x=0.3

The flash points and vapor pressures of several solvents and their electrolytes with a lithium salt molecular ratio x=0.3 are presented in Table 1 below. It may be noted that, according to the OSHA (Occupational Safety & Health Administration) classification, any liquid with a flash point below 38.7° C. is flammable. However, in order to ensure safety, we have designed our quasi-solid electrolytes to exhibit a flash point significantly higher than 38.7° C. (by a large margin, e.g. at least increased by 50° and preferably above 150° C.). The data in Table 1 indicate that the addition of a lithium salt to a molecular ratio of 0.35 is normally sufficient to meet these criteria.

TABLE 1

The flash points and vapor pressures of select solvents and their electrolytes with a lithium salt molecular ratio x = 0.3.

Chemical	Flash point (° C.)	Flash point (° C.) with x = 0.35 of (Li salt)	Vapor pressure (kPa) at 20° C.	Vapor pressure (kPa) at 20° C. with x = 0.35
Acetone	−17	—	24 kPa (240 hPa)	—
Ethanol	17	—		—
Gasoline	−42	—		—
Canola oil	327	—		—
DOL (1,3-dioxolane)	1	75 ($LiBF_4$)	9.33 (70 Torr)	2.6 ($LiBF_4$)
DOL	1	155 ($LiCF_3SO_3$)	9.33	0.8 ($LiCF_3SO_3$)
DEC (diethyl carbonate)	33	>200 ($LiCF_3SO_3$)	1.33 (10 Torr)	0.09 ($LiCF_3SO_3$)
DMC (Dimethyl carbonate)	18	177 ($LiCF_3SO_3$)	2.40 (18 Torr)	0.13 ($LiCF_3SO_3$)
EMC (ethyl methyl carbonate)	23	188 (LiBOB)	3.60 (27 Torr)	0.1 (LiBOB)
EC (ethylene carbonate)	145	No flash point (LiBOB)	<0.0013 (0.02 Torr at 36.4° C.)	<0.01 (LiBOB)
PC (propylene carbonate)	132	No flash point (LiBOB)	0.0173 (0.13 Torr)	<0.01 (LiBOB)
γ-BL (gamma-butyrolactone),	98	No flash point (LiBOB)	0.20 (1.5 Torr)	<0.01 (LiBOB)
AN (Acetonitrile)	6	85 ($LiBF_4$)	9.71 (88.8	1.5 ($LiBF_4$)

TABLE 1-continued

The flash points and vapor pressures of select solvents and their
electrolytes with a lithium salt molecular ratio x = 0.3.

Chemical	Flash point (° C.)	Flash point (° C.) with x = 0.35 of (Li salt)	Vapor pressure (kPa) at 20° C.	Vapor pressure (kPa) at 20° C. with x = 0.35
			Torr at 25° C.)	
EA (Ethyl acetate) + DOL	−3	70 (LiBF$_4$)	9.73	1.3 (LiBF$_4$)
DME (1,2-dimethoxyethane)	−2	66 (LiPF$_6$)	6.40 (48 Torr)	2.1 (LiPF$_6$)
VC (vinylene carbonate)	53.1	155 (LiPF$_6$)	11.98 (89.9 Torr)	0.9 (LiPF$_6$)
TEGDME (tetraethylene glycol dimethylether)	141	No flash point (LiPF$_6$)	<0.0013 (<0.01 Torr)	<0.001
FEC (Fluoro ethylene carbonate)	122	No flash point (LiPF$_6$)	0.021	<0.01
FPC (Trifluoro propylene carbonate)	No flash point	No flash point (LiPF$_6$)	—	—
HFEs (TPTP) hydrofluoro ether	No flash point	No flash point (LiPF$_6$)	0.7	<0.1
MFE (methyl nonafluorobutyl ether)	No flash point	No flash point (LiPF$_6$)	—	—
IL (1-ethyl-3-methyl imadazolium TFSI)	283	No flash point (LiTFSI)	—	—

* As per OSHA (Occupational Safety & Health Administration) classification, any liquid with a flash point below 38.7° C. is flammable.
** 1 standard atmosphere = 101,325 Pa = 101.325 kPa = 1,013.25 hPa. 1 Torr = 133.3 Pa = 0.1333 kPa

Example 4: Lithium Ion Transference Numbers in Several Electrolytes

The Li$^+$ ion transference numbers of several types of electrolytes (e.g. LiTFSI salt/(EMImTFSI+DME) solvents) in relation to the lithium salt molecular ratio were studied and representative results are summarized in FIG. **5-8**. In general, the Li$^+$ ion transference number in low salt concentration electrolytes decreases with increasing concentration from x=0 to x=0.2-0.35. However, beyond molecular ratios of x=0.2-0.35, the transference number increases with increasing salt concentration, indicating a fundamental change in the Li$^+$ ion transport mechanism. This was explained in the theoretical sub-sections earlier. When Li$^+$ ions travel in a low salt concentration electrolyte (e.g. x<0.2), a Li$^+$ ion can drags multiple solvating anions or molecules along with it. The coordinated migration of such a cluster of charged species can be further impeded if the fluid viscosity is increased due to more salt dissolved in the solvent. In contrast, when an ultra-high concentration of lithium salt with x>0.2 is present, Li$^+$ ions could significantly out-number the available solvating anions that otherwise could cluster the lithium ions, forming multi-ion complex species and slowing down their diffusion process. This high Li$^+$ ion concentration makes it possible to have more "free Li$^+$ ions" (non-clustered), thereby providing a higher Li$^+$ transference number (hence, a facile Li$^+$ transport). The lithium ion transport mechanism changes from a multi-ion complex-dominating one (with an overall larger hydrodynamic radius) to single ion-dominating one (with a smaller hydrodynamic radius) having a large number of available free Li$^+$ ions. This observation has further asserted that an adequate number of Li$^+$ ions can quickly move through or from the quasi-solid electrolytes to make themselves readily available to interact or react with a cathode (during discharge) or an anode (during charge), thereby ensuring a good rate capability of a lithium secondary cell. Most significantly, these highly concentrated electrolytes are non-flammable and safe. Combined safety, facile lithium ion transport, and electrochemical performance characteristics have been thus far difficult to come by for all types of lithium secondary battery.

Example 5: Exfoliated Graphite Worms from Natural Graphite Using Hummers Method

Graphite intercalation compound (GIC) was prepared by intercalation and oxidation of natural graphite flakes (original size of 200 mesh, from Huadong Graphite Co., Pingdu, China, milled to approximately 15 μm) with sulfuric acid, sodium nitrate, and potassium permanganate according to the method of Hummers [U.S. Pat. No. 2,798,878, Jul. 9, 1957]. In this example, for every 1 gram of graphite, we used a mixture of 22 ml of concentrated sulfuric acid, 2.8 grams of potassium permanganate, and 0.5 grams of sodium nitrate. The graphite flakes were immersed in the mixture solution and the reaction time was approximately three hours at 30° C. It is important to caution that potassium permanganate should be gradually added to sulfuric acid in a well-controlled manner to avoid overheat and other safety issues. Upon completion of the reaction, the mixture was poured into deionized water and filtered. The sample was then washed repeatedly with deionized water until the pH of the filtrate was approximately 5. The slurry was spray-dried and stored in a vacuum oven at 60° C. for 24 hours. The resulting GIC was exposed to a temperature of 1,050° C. for 35 seconds in a quartz tube filled with nitrogen gas to obtain worms of exfoliated graphite flakes.

Example 6: Conductive Web of Filaments from Electro-Spun PAA Fibrils for Anode

Poly (amic acid) (PAA) precursors for spinning were prepared by copolymerizing of pyromellitic dianhydride (Aldrich) and 4,4'-oxydianiline (Aldrich) in a mixed solvent of tetrahydrofurane/methanol (THF/MeOH, 8/2 by weight). The PAA solution was spun into fiber web using an electrostatic spinning apparatus. The apparatus consisted of a 15 kV d.c. power supply equipped with the positively charged capillary from which the polymer solution was extruded, and a negatively charged drum for collecting the fibers. Solvent removal and imidization from PAA were performed concurrently by stepwise heat treatments under air flow at 40° C. for 12 h, 100° C. for 1 h, 250° C. for 2 h, and 350° C. for 1 h. The thermally cured polyimide (PI) web samples

were carbonized at 1,000° C. to obtain a sample with an average fibril diameter of 67 nm. Such a web can be used to accommodate sulfur (or lithium polysulfide), vanadium oxide, titanium disulfide, etc., for the cathode and/or as a conductive substrate for an anode active material.

Example 7: Preparation of NGP-Based Webs (Webs of NGPs and NGPs+CNFs) for the Anode or Cathode (as a Conductive Nanostructured Support)

The starting natural graphite flakes (original size of 200 mesh, from Huadong Graphite Co., Pingdu, China) was milled to approximately 15 μm. The intercalation and oxidation chemicals used in the present study, including fuming nitric acid (>90%), sulfuric acid (95-98%), potassium chlorate (98%), and hydrochloric acid (37%), were purchased from Sigma-Aldrich and used as received.

A reaction flask containing a magnetic stir bar was charged with sulfuric acid (360 mL) and nitric acid (180 mL) and cooled by immersion in an ice bath. The acid mixture was stirred and allowed to cool for 15 min, and graphite particles (20 g) were added under vigorous stirring to avoid agglomeration. After the graphite particles were well dispersed, potassium chlorate (110 g) was added slowly over 15 min to avoid sudden increases in temperature. The reaction flask was loosely capped to allow evolution of gas from the reaction mixture, which was stirred for 48 hours at room temperature. On completion of the reaction, the mixture was poured into 8 L of deionized water and filtered. The slurry was spray-dried to recover an expandable graphite sample. The dried, expandable graphite sample was quickly placed in a tube furnace preheated to 1,000° C. and allowed to stay inside a quartz tube for approximately 40 seconds to obtain exfoliated graphite worms. The worms were dispersed in water to form a suspension, which was ultrasonicated with a power of 60 watts for 15 minutes to obtain separated NGPs.

Approximately half of the NGP-containing suspension was filtered and dried to obtain several paper-like mats. Vapor grown CNFs were then added to the remaining half to form a suspension containing both NGPs and CNFs (20%), which was dried and made into several paper-like mats. Approximately 5% phenolic resin binder was used to help consolidate the web structures in both samples. Such a web can be used as a conductive substrate for an anode active material.

Example 8: Impregnation of Se or Se/S in Meso-Porous Graphite Worm Conductive Structures for Li—Se or Li—Se/S Cathodes

In a typical procedure, a meso-porous graphite worm structure or a nano-filament web and solid selenium or selenium/sulfur powder are sealed in a stainless steel crucible and heated to a temperature of 221-250° C. The molten Se or Se/S material was allowed to permeate into the pores of the porous nano-structure for typically from 2 to 20 minutes. The coating thickness was varied by varying the amount of Se or Se/S material incorporated and the impregnation time. A Se/S coating thickness lower than 100 nm is preferred, but more preferred is a thickness lower than 20 nm, and most preferred is a thickness lower than 10 nm (or even 5 nm). Several lithium metal cells with or without a nano-structured anode were fabricated, wherein a lithium metal foil was used as a source of Li^+ ions at the anode.

It may be noted that both Se and S have a relatively low melting points, both lower than 221° C. and, hence, homo-geneous mixing of Se and S can be readily achieved using melt mixing techniques. Complete solution of Se in S or S in Se can be obtained at any atomic ratio or weight ratio between Se and S. Such a characteristic gives us the flexibility in producing cathode active materials of various compositions consisting of both Se and S (not S alone).

Example 9: Mixing of Se or Se/S with Graphene or CNF Powders Using Ball Milling

Mixtures of solid selenium or selenium/sulfur powder with either graphene powder or carbon nano-fibers (CNFs), at various proportions, were separately sealed in ball mill chambers and subjected to ball-milling in a planetary ball mill for a period of time, typically 1-4 hours. We have also observed that complete mixing between Se and S can be achieved with ball milling at any Se/S ratio.

Several dry electrodes containing graphene-enhanced particulates or CNF-enhanced particles (e.g. comprising Se or Se/S primary particles embraced by graphene sheets or blended with CNFs) were prepared by mixing the particulates with a liquid to form a paste with or without using a binder such as PVDF. The paste was cast onto a surface of a piece of glass, with the liquid medium removed to obtain a dry electrode.

Example 10: Evaluation of Electrochemical Performance of Various Cells

Charge storage capacities were measured periodically and recorded as a function of the number of cycles. The specific discharge capacity herein referred to is the total charge inserted into the cathode during the discharge, per unit mass of the composite cathode (counting the weights of cathode active material, conductive additive or support, binder, and any optional additive combined, but excluding the current collector). The specific charge capacity refers to the amount of charges per unit mass of the composite cathode. The specific energy and specific power values presented in this section are based on the total cell weight. The morphological or micro-structural changes of selected samples after a desired number of repeated charging and recharging cycles were observed using both transmission electron microscopy (TEM) and scanning electron microscopy (SEM).

As an example, the cycling performance (discharge specific capacity) of a Li metal-selenium (Li—Se) cell containing a low-concentration electrolyte (1 M of lithium salt in an organic liquid) and that of a corresponding cell containing a quasi-solid electrolyte (4 M) are shown in FIG. 10. In both cells, the cathode contains 15% CNT as a conductive additive. It is quite clear that the capacity of the conventional low-concentration electrolyte cell rapidly decays as charges and discharges are repeated, suffering a 31% capacity loss after 500 cycles. This is characteristic of conventional Li—Se and Li—S cells that have great propensity for sulfur, lithium polysulfide, or lithium polyselenide to get dissolved in the electrolyte at the cathode side. Much of the dissolved species could not be re-deposited to the cathode conductive additive/substrate or the cathode current collector during subsequent charges/discharges. Most critically, as time goes on or when charge/discharge cycling continues, some of the dissolved lithium polysulfide or polyselenide species migrate to the anode side and react with Li to form insoluble products and, hence, these species could not return to the cathode. These phenomena lead to continuing decay in the battery capacity. In contrast, with a quasi-solid electrolyte, these issues appear to be significantly reduced or eliminated

and the cell experiences a capacity loss of only 10% after 1,000 cycles. This by itself is a great achievement in the field of Li—Se batteries.

During the initial phase of our research efforts on quasi-solid electrolytes, we encountered some major challenges. First, we did not have a wide range of lithium salt concentrations at our disposal. Most of the lithium salts could not be dissolved in those solvents commonly used in Li-ion, Li—S or Li—Se secondary cells for more than a molar ratio of 0.2-0.3. Second, we quickly came to realize that the viscosity of many organic liquid solvents was already extremely high at room temperature and adding more than 0.2-0.3 molar ratio of a lithium salt in such a viscous solid made the resulting mixture look like and behave like a solid. It was next to impossible to use a stirrer to help disperse the solid lithium salt powder in the liquid solvent. Further, a higher solute concentration was generally believed to be undesirable since a higher concentration normally would result in a lower lithium ion conductivity in the electrolyte. This would not be conducive to achieving a higher power density, lower polarization, and higher energy density (at high charge/discharge rates). We almost gave up, but decided to move forward anyway and the research results have been most surprising.

Contrary to the expectations by electrochemists and battery designers that a significantly higher lithium salt concentration could not be produced, we found that a concentration as high as $x=0.2$-0.6, roughly corresponding to 3-11 M of a lithium salt in some organic liquid could be achieved, if a highly volatile solvent (such as AN or DOL) is added as a co-solvent first. Once a complete dissolution of a lithium salt in a mixture solvent is attained, we could choose to selectively remove the co-solvent. We were pleasantly surprised to observe that partial or complete removal of the more volatile co-solvent upon complete salt dissolution would not result in crystallization or precipitation of the salt from the organic liquid solvent even though the salt (a solute) was then in a highly supersaturated condition.

We have further defied the expectation of battery chemists and engineers that a higher electrolyte concentration would lead to a lower discharge capacity. Most surprisingly, the lithium-selenium cells containing a higher-concentration electrolyte system exhibit not only a generally higher energy density but also a dramatically more stable cycling behavior and longer cycle life.

As another example, FIG. 10 shows the discharge specific capacity of 4 Li—SeS$_7$ cells: two containing an organic liquid solvent-based quasi-solid electrolyte (5 M) and the other two containing a conventional electrolyte (1 M). Each cell has either a graphene (NGP) nanostructure or a carbon nano-fiber (CNF) nanostructure to support the cathode active material (SeS$_7$ alloy in this example). The cycling performance of the cell having a quasi-solid electrolyte is so much better than that of the corresponding cell having a lower salt concentration, for both NGP and CNF supported

cells. Further, the NGP-supported cathode appears to be significantly more effective in imparting cycling stability to the Li—Se/S cell.

FIG. 11 shows the Ragone plots (cell power density vs. cell energy density) of two Li-ion Se/S cells each having a prelithiated Si nano particle anode and a graphene-supported Se$_2$S$_3$ alloy cathode, but the lithium salt concentrations being 1 M and 6M, respectively. Not only the energy density, but also the power density of the Li-ion Se/S cell is improved when the organic liquid-based solvent has a much higher lithium salt concentration. This is completely opposite to the expectations of electrochemists and battery designers that (1) organic liquids should not be capable of dissolving more than $x=0.2$ or approximately >3.5 M of lithium salt; and (2) with a higher salt concentration, the electrolyte viscosity should be even higher, making the lithium ions even less mobile with a lower diffusion coefficient and, hence, leading to a reduced lithium ion migration rate and reduced power density. A logical question to ask is why a higher electrolyte concentration (higher than 3.5 M) seems to allow for a facile transport of lithium ions, Li$^-$. The answers are briefly repeated below:

When lithium ions are formed in the conventional lower-concentration electrolyte, the positively charged lithium ions Li$^+$ might be associated with or surrounded by the solvating anions or molecules that help to dissolve or "solvate" the Li$^+$ ions. Typically, one Li$^+$ ion can be clustered with several (2-4) solvating species. In other words, when a Li$^+$ ion moves, it has to drag along several molecules to move with it. Such a Li$^+$ ion transport mechanism would be very sensitive to the variation in electrolyte viscosity, which would increase with increasing lithium salt concentration and decreasing temperature. In contrast, with a much higher lithium salt concentration, there would be significantly more Li$^+$ ions than the solvating molecules in the electrolyte. Consequently, many of the Li$^+$ ions become "free" ions when the lithium salt concentration is sufficiently high. These free Li$^+$ ions could move faster than if they were clustered with solvating anions as in the electrolyte of a low salt concentration. It seems that when the lithium salt concentration is greater than $x=0.2$, the free Li$^+$ ions would significantly outnumber the solvated Li$^+$ ions, and the number of free Li$^+$ ions would also be greater than the total number of Li$^+$ ions (regardless if they are clustered with solvating molecules or not) in an electrolyte having a concentration$<x=0.1$.

Example 11: The Effect of Lithium Salt
Concentration on the Capacity Fade and Cathode
Active Material Utilization Rate of Various
Lithium-Selenium Cells

Additional data on the correlation between electrochemical performance of various Li—Se/S metal cells and Li-ion Se/S cells with the lithium salt concentration are presented in Table 2 below.

TABLE 2

						Capacity	Cathode
						loss	active
Cell				Anode	Cathode	after 50	material
ID	Solvent(s)	Li salt (solute)	x	active material	active material	cycles	utilization rate
N-1	TPTP + DOL	(LiN(CF$_3$SO$_2$)$_2$	0.08	Li metal	30% S +	58%	56%
N-2	(ratio = 7:1)		1.6		20% Se +	40%	97%

Examples of the electrolytes and lithium salt concentrations used.

TABLE 2-continued

Cell ID	Solvent(s)	Li salt (solute)	x	Anode active material	Cathode active material	Capacity loss after 50 cycles	Cathode active material utilization rate
N-3			0.38		50% CB	2.5%	66%
N-4			0.46			0%	68%
K-1	TPTP +	$(LiN(CF_3SO_2)_2)$	0.11	Li metal	60% Se +	8.5%	84%
K-2	TEGDME		0.33		20% S +	1.1%	86%
K-3	(ratio = 6:1)		0.42		20% EG	0%	91%
K-4			0.51			0%	93%
P-1	DME	$LiCF_3SO_3$	0.08	Li metal	80% SeS$_2$ +	10%	70%
P-2			0.31		20% CNT	2.3%	80%
P-3			0.41			0.3%	84%
Q-1	DME	LiBOB	0.15	Lithiated	80% SeS$_2$ +	4.6%	81%
Q-2			0.21	Si nano-	20% EG	2.4%	87%
Q-3			0.26	particles		1.5%	89%
Q-4			0.33			0.9%	92%
R-1	DMC +	LiTFSI	0.07	Li metal	80% SsS$_2$ +	10%	76%
R-2	BEPyTFSI (ratio = 10:1)		0.27		20% NGP	3.4%	89%

Based on the data as summarized in Table 1, one can make the following significant observations: (a) The higher-concentration electrolyte results in a dramatically better battery cycling performance (higher capacity retention rate or lower capacity loss) and a higher cathode active material utilization rate, as compared to the lower-concentration electrolyte. (b) In addition to the implementation of a higher concentration electrolyte system, a meso-porous or porous nano-structured cathode supporting network composed of exfoliation graphite worms (EGW) or other types of conductive nano-filaments, such as carbon nanotubes (CNTs) and graphene (NGPs), further improves the cycling stability and active material utilization rate in a rechargeable Li-SE/s cell. Among these conductive network structures, EGWs and NGP appear to provide best overall performance.

Example 12: Significant Impact of the Present Invention to Society

The energy density and power density data of two Li—SeS$_2$ cells having an exfoliated graphite worm-supported SeS$_2$ alloy as the cathode are summarized in the Ragone plots of FIG. 12. One cell has a conventional low-concentration electrolyte (1 M) and the other a quasi-solid electrolyte (5 M). There are several significant observations that can be made from these data:

(a) The energy density of the Li—SeS$_2$ cell containing a quasi-solid electrolyte reaches a value of 662 Wh/kg, which is 3 to 4 times higher than the energy density (typically in the range of 150-200 Wh/g) of lithium-ion cells. A quasi-solid electrolyte again imparts significantly higher energy density and power density to the battery cell as compared to its conventional low-concentration electrolyte counterpart.

(b) The same cell can deliver a maximum power density of 5,253 W/kg, which is one order of magnitude higher than the power density of lithium-ion batteries (typically 300-500 W/kg). This high power density implies a battery capable of being charged and discharged at a high rate. Such a high power density, comparable to those of a supercapacitor, also enables this Li—SeS$_2$ battery to be used in situations where pulse power and/or fast energy-capturing capability are required (e.g. for recuperating the kinetic energy of a vehicle during deceleration and providing the required pulse power during acceleration).

(c) A three-fold increase in energy density is also expected to have a highly positive impact to society (e.g. in terms of reducing carbon dioxide emission if EV industry emerges). Currently, the primary barriers against more widespread acceptance of battery-powered EVs by consumers are that the EV batteries are still too expensive and too heavy, and there are very few battery charging stations available in any country. For instance, the battery in GM Volt is designed to run on the battery for a distance of 40 miles, and Nissan Leaf for 120 miles. These battery-only ranges are clearly not enough for a typical driver who is so accustomed to driving a gasoline-powered car for 300 miles without having to re-fill the gasoline tank. As an alternative, the high-end all electric vehicle (e.g. S-model manufactured by Tesla Motors, Santa Clara, Calif.) operates on a 85-kwh (kilo watt-hour) lithium battery system that can run for 350 miles on one battery charge. However, the battery system weights almost 1,800 pounds, occupies the entire chassis of the car, and today costs about $60,000-$75,000 (battery system alone). This battery cost is equivalent to approximately $700-800 per kWh. The US Department of Energy believes that the EV industry cannot be economically viable unless the battery cost goes below $250/kWh.

These high cost and heavy weight problems associated with current lithium-ion batteries are due to a major shortcoming of lithium-ion batteries: low energy density (low amount of energy stored in a given battery weight, resulting in an insufficient battery-only driving distance on one battery charge). To meet this challenging goal, the energy density of an EV battery must be increased from the current 150 Wh/kg to at least 450 Wh/kg without significantly increasing the battery system costs. This would reduce the battery system cost from approximately $750/kWh to $250/kWh. The presently invented battery system with quasi-solid electrolyte can deliver an energy density three to four times higher than that of a conventional Li-ion battery at a comparable or reduced cost, leading to a battery system cost of <$250/kWh. Given the same battery system

weight, the EV featuring the presently invented Li—Se/S cell can run for 1,000 miles between two battery charges, reducing the need to build extensive charging station infrastructure. Alternatively, with the same 85 kWh of energy, the battery system weight can be reduced by a factor of 3 (e.g. down to <600 pounds or 280 kg). Clearly, the instant invention can potentially help to accelerate the emergence of a vibrant EV industry and helping society to better cope with environmental issues associated with gasoline-powered vehicles.

In summary, the present invention provides an innovative, versatile, and surprisingly effective platform materials technology that enables the design and manufacture of superior lithium metal and lithium-ion rechargeable batteries based on Se or Se/S cathodes. The lithium cell featuring a high-concentration electrolyte system exhibits a stable and safe anode (no dendrite-like feature), high lithium utilization rate, high cathode active material utilization rate, high specific capacity, high specific energy, high power density, little or no shuttling effect, and long cycle life. We have further observed that the electrochemical performance of lithium secondary cells containing, as electrolyte, a high concentration of lithium salt dissolved in an organic liquid solvent is relatively independent of the battery operating temperature and the cells can effectively operate in an unusually wide temperature range, extending to a very low temperature and a very high temperature regime. This temperature range is the widest among all known lithium batteries.

The presently invented cells can provide a specific energy greater than 400 Wh/Kg (more typically greater than 500 Wh/Kg, and often greater than 600 Wh/Kg, based on the total cell weight including anode, cathode, electrolyte, separator, and current collector weights combined. This has not been achieved by any prior art approaches.

The invention claimed is:

1. A rechargeable lithium-selenium cell comprising a cathode having a cathode active material selected from Se or Se_xS_y (x/y ratio=0.01 to 100), an anode having an anode active material, a porous separator electronically separating said anode and said cathode, a non-flammable quasi-solid electrolyte in contact with said cathode and said anode, wherein said electrolyte consists essentially of a lithium salt dissolved in a first organic liquid solvent with a lithium salt concentration greater than 3.5 M wherein said electrolyte is in a supersaturated state without precipitation or crystallization of the lithium salt out of the liquid solvent and most of said solvent molecules are retained or captured by said lithium salt ions that are not volatile so that said electrolyte exhibits a vapor pressure less than 0.01 kPa when measured at 20° C., a vapor pressure less than 60% of the vapor pressure of said first organic solvent alone, a flash point at least 20 degrees Celsius higher than a flash point of said first organic liquid solvent alone, a flash point higher than 150° C., or no flash point, and wherein said electrolyte contains no ionic liquid solvent.

2. The rechargeable lithium-selenium cell of claim 1, wherein said lithium salt concentration is greater than 5.0 M or greater than a molar fraction of 0.5.

3. The rechargeable lithium-selenium cell of claim 1, wherein said lithium salt concentration is greater than 7.0 M or greater than a molar fraction of 0.6.

4. The rechargeable lithium-selenium cell of claim 1, wherein said electrolyte has a lithium ion transference number greater than 0.4.

5. The rechargeable lithium-selenium cell of claim 1, wherein said electrolyte has a lithium ion transference number greater than 0.75.

6. The rechargeable lithium-selenium cell of claim 1, wherein said electrolyte has a lithium ion transference number greater than 0.6.

7. The rechargeable lithium-selenium cell of claim 1, wherein said first organic liquid solvent is selected from the group consisting of 1,3-dioxolane (DOL), 1,2-dimethoxy-ethane (DME), tetraethylene glycol dimethylether (TEGDME), poly(ethylene glycol) dimethyl ether (PEGDME), diethylene glycol dibutyl ether (DEGDBE), 2-ethoxyethyl ether (EEE), sulfone, sulfolane, ethylene carbonate (EC), dimethyl carbonate (DMC), methylethyl carbonate (MEC), diethyl carbonate (DEC), ethyl propionate, methyl propionate, propylene carbonate (PC), gamma butyrolactone (γ-BL), acetonitrile (AN), ethyl acetate (EA), propyl formate (PF), methyl formate (MF), toluene, xylene, methyl acetate (MA), fluoroethylene carbonate (FEC), vinylene carbonate (VC), allyl ethyl carbonate (AEC), a hydrofluoroether, and combinations thereof.

8. The rechargeable lithium-selenium cell of claim 1, wherein said lithium salt is selected from lithium perchlorate $(LiClO_4)$, lithium hexafluorophosphate $(LiPF_6)$, lithium borofluoride $(LiBF_4)$, lithium hexafluoroarsenide $(LiAsF_6)$, lithium trifluoro-metasulfonate $(LiCF_3SO_3)$, bis-trifluoromethyl sulfonylimide lithium $(LiN(CF_3SO_2)_2)$, lithium bis (oxalato)borate (LiBOB), lithium oxalyldifluoroborate $(LiBF_2C_2O_4)$, lithium oxalyldifluoroborate $(LiBF_2C_2O_4)$, lithium nitrate $(LiNO_3)$, Li-Fluoroalkyl-Phosphates $(LiPF_3 (CF_2CF_3)_3)$, lithium bisperfluoro-ethysulfonylimide (Li-BETI), lithium bis(trifluoromethanesulphonyl)imide, lithium bis(fluorosulphonyl)imide, lithium trifluoromethanesulfonimide (LiTFSI), an ionic liquid lithium salt, or a combination thereof.

9. The rechargeable lithium cell of claim 1 wherein said anode contains an anode active material selected from lithium metal, a lithium metal alloy, a mixture of lithium metal or lithium alloy with a lithium intercalation compound, a lithiated compound, lithiated titanium dioxide, lithium titanate, lithium manganate, a lithium transition metal oxide, $Li_4Ti_5O_{12}$, or a combination thereof.

10. The rechargeable lithium cell of claim 1 wherein said anode contains an anode active material selected from the group consisting of:
    (a) lithiated versions of silicon (Si), germanium (Ge), tin (Sn), lead (Pb), antimony (Sb), bismuth (Bi), zinc (Zn), aluminum (Al), nickel (Ni), cobalt (Co), manganese (Mn), titanium (Ti), iron (Fe), and cadmium (Cd);
    (b) lithiated versions of alloys or intermetallic compounds of Si, Ge, Sn, Pb, Sb, Bi, Zn, Al, or Cd with other elements, wherein said alloys or compounds are stoichiometric or non-stoichiometric;
    (c) lithiated versions of oxides, carbides, nitrides, sulfides, phosphides, selenides, and tellurides of Si, Ge, Sn, Pb, Sb, Bi, Zn, Al, Fe, Ni, Co, Ti, Mn, or Cd, and their mixtures or composites;
    (d) lithiated versions of salts and hydroxides of Sn;
    (e) lithiated versions of carbon or graphite materials; and combinations thereof.

11. The rechargeable lithium-selenium cell of claim 1, wherein the x/y ratio in Se_xS_y is from 0.05 to 20.

12. The rechargeable lithium-selenium cell of claim 1, wherein Se_xS_y is selected from Se_5S, Se_5S_2, Se_5S_4, SeS, Se_3S_5, SeS_2, SeS_7, or SeS_z, where z is from 7 to 20.

13. The rechargeable lithium-selenium cell of claim **1**, wherein said cathode active material contains Se and lithium-selenium cell is a Li—Se cell.

14. The rechargeable lithium-selenium cell of claim **1**, wherein said anode active material is supported by a network of conductive nano filaments selected from carbon nano-tubes, carbon nano-fibers, graphene sheets, exfoliated graphite flakes, carbon black, or a combination thereof.

15. A rechargeable lithium-selenium cell, comprising a cathode having a cathode active material selected from Se or Se_xS_y (x/y ratio=0.01 to 100), an anode having an anode active material, a porous separator electronically separating said anode and said cathode, a non-flammable quasi-solid electrolyte in contact with said cathode and said anode, wherein said cathode active material is supported by a network of conductive nano filaments selected from carbon nano-tubes, carbon nano-fibers, graphene sheets, exfoliated graphite flakes, carbon black, or a combination thereof, and wherein said electrolyte contains a lithium salt dissolved in a first organic liquid solvent with a lithium salt concentration greater than 5.0 M wherein said electrolyte is in a super-saturated state wherein most of said solvent molecules are retained or captured by said lithium salt ions that are not volatile and said electrolyte further contains an ionic liquid solvent and a first organic liquid solvent-to-ionic liquid solvent ratio is greater than 1/1.

16. The rechargeable lithium cell of claim **15**, wherein said ionic liquid solvent is selected from a room temperature ionic liquid having a cation selected from tetraalkylammonium, di-, tri-, or tetra-alkylimidazolium, alkylpyridinium, dialkyl-pyrrolidinium, dialkylpiperidinium, tetraalkylphosphonium, trialkylsulfonium, or a combination thereof.

17. The rechargeable lithium cell of claim **15**, wherein said ionic liquid solvent is selected from a room temperature ionic liquid having an anion selected from BF_4^-, $B(CN)_4^-$, $CH_3BF_3^-$, $CH_2CHBF_3^-$, $CF_3BF_3^-$, $C_2F_5BF_3^-$, n-$C_3F_7BF_3^-$, n-$C_4F_9BF_3^-$, PF_6^-, $CF_3CO_2^-$, $CF_3SO_3^-$, $N(SO_2CF_3)_2^-$, $N(COCF_3)(SO_2CF_3)^-$, $N(SO_2F)_2^-$, $N(CN)_2^-$, $C(CN)_3^-$, SCN^-, $SeCN^-$, $CuCl_2^-$, $AlCl_4^-$, $F(HF)_{2.3}^-$, or a combination thereof.

18. A rechargeable lithium-selenium cell comprising a cathode having a cathode active material selected from Se or Se_xS_y (x/y ratio=0.01 to 100), an anode having an anode active material, a porous separator electronically separating said anode and said cathode, a non-flammable quasi-solid electrolyte in contact with said cathode and said anode, wherein said cathode active material is supported by a network of conductive nano filaments selected from carbon nano-tubes, carbon nano-fibers, graphene sheets, exfoliated graphite flakes, carbon black, or a combination thereof and said electrolyte contains a lithium salt dissolved in a first organic liquid solvent with a lithium salt concentration higher than 3.5 M wherein said electrolyte is in a supersaturated state without precipitation or crystallization of the lithium salt out of the liquid solvent and most of said solvent molecules are retained or captured by said lithium salt ions that are not volatile so that said electrolyte exhibits a vapor pressure less than 0.02 kPa when measured at 20° C., a vapor pressure less than 60% of the vapor pressure of said first organic solvent alone, a flash point at least 20 degrees Celsius higher than a flash point of said first organic liquid solvent alone, a flash point higher than 150° C., or no flash point.

* * * * *